Facultad
de
Ciencias

Electromagnetic behavior of nanoparticle dimers.
(Comportamiento electromagnético de dímeros de nanopartículas)

Trabajo de Fin de Grado
para acceder al

GRADO EN FÍSICA

Autor: Ángela Barreda Gómez

Director: Francisco González Fernández

Co-Director: Fernando Moreno Gracia

Junio - 2013

Agradecimientos:

Me gustaría expresar mi agradecimiento a Fernando y Paco por haberme dirigido el proyecto y haberme dedicado buena parte de su tiempo. A Rodrigo por todo lo que me ha enseñado. A Juanma, Lola y Chema por su interés en mi trabajo y por su buena disposición.

Dedicatoria:

A mis padres por todo; a mis abuelos, especialmente a mi abuelo Paco; y a Óscar.

Index

1.1 Plasmonics

The interaction of electromagnetic radiation with matter is a very active field in different branches of physics. Its study has provided results in diverse areas like medicine, spectroscopy, optics…The way of understanding and explaining this phenomenon has progressed in time, as it is usual in science.

Nanophotonics is the study of interaction between electromagnetic radiation and matter to nanometric scale. Surprising properties that exhibit these tiny structures when they are illuminated with light, have supposed a new research topic. Concretely, small spherical particles, (nanoparticles), have been used in many applications.

One of the most important branches of metallic optics is plasmonics. Its study is based on plasmons, collective oscillations of the free electrons that constitute a metal, when it is illuminated with electromagnetic radiation. We can distinguish two kind of plasmons: surface plasmons and localized surface plasmons, their characteristics will be explained in the following sections: 1.2-1.3.

In cases in which the dimensions of the metallic structure are in the range of nanometers, we can talk about nanoplasmonics. When the plasmonics resonance is produced, energy of incident electromagnetic wave is transferred to nanoparticles that constitute the system, then, big concentrations of electromagnetic energy appear around the nanostructure surface. Those concentrations make this study interesting and provide possible applications in biosensing manufacturing, microscopy, solar cells…

At the beginning, published papers were based on the study of metallic nanoparticles due to good response that these structures show when they are excited with radiation in visible range. However, in this kind of materials, incident light may be absorbed and as a consequence, Joule´s losses should be considered. For last few years, new structures have been developed by using dielectric nanoparticles with high refractive index, these materials, depending on their size and shape, show clear resonances in different spectral ranges. Because of that light can travel through them without being absorbed and that they present directionality properties, they are used in many applications, for example as nanoantennas, as it will be commented in section 9.

In this project we have intended to advance in the knowledge of new systems where big concentrations of electromagnetic energy are produced, with potential applications in nanoantennas, SERS technique…Concretely, we have studied the simplest system in which multiple interaction effects are present: dimer. For finding out the solution we have used numerical methods, because it is impossible to solve this problem in an analytic way. However, for the case of an isolated particle, Mie in 1908 provided an analytical solution to the problem of scattering and absorption of light by spherical particles. Also, this theory is valid for metallic and dielectric nanoparticles.

1.2 Surface plasmons

One of the most important properties in metals is that, in addition to being able to reflect light, verifying some conditions, this can propagate by the metallic surface without leaving it, creating surface plasmons (figure 1.1). They are present in the interface between a dielectric and a metal if there is a different sign in the real dielectric constant of both mediums, in general we consider a metal with negative dielectric constant and a dielectric with positive optics constants, and if the wave vectors of incident radiation and plasmons are equal. The most surprising fact is that they are able to confine electromagnetic energy on a surface, in most of cases it travels in space (three dimensions). This property is due to presence of free electrons in metal.

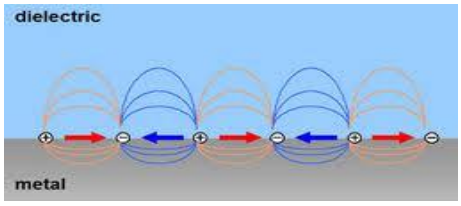

Figure 1.1: *surface Plasmon.*

The wave vector of plasmons is given by the following equation:

$$k = \frac{\omega}{c}\sqrt{\frac{\varepsilon_1 \varepsilon_2}{\varepsilon_1 + \varepsilon_2}} \tag{1.1}$$

Where ε_1 and ε_2 are the relative dielectric constants of the metal and dielectric respectly, ω is the frequency of wave and c is the speed of light in vacuum. [1]

Through the expression (1.1) we can observe as the wave vector of plasmons is always bigger than the wave vector of light. For this reason, in order to excite surface plasmons using photons, it is necessary to draw on one of the following methods: waveguides, grating coupler and attenuated total reflectance.

1.3 Localized surface plasmons

In metals, it is known that there are lots of free electrons, even to low temperature. Because of that, they are good electrical and thermal conductors.

One of the simplest models that is able to provide reliable results and to explain the behavior of metals from a microscopic point of view, but attending to classic arguments, is the Drude model.

When metallic nanoparticles are illuminated by electromagnetic radiation, the electron cloud starts to oscillate to the same frequency as incident wave. These coherent oscillations of electronic plasma, localized surface plasmons, depending on the optical properties, the particle size, shape and the wavelength of light originate different surface charge distributions. [2]

If the particle size comparison with wavelength is small, the charge distribution will be dipolar. The incident field, considered as a plane wave, varies in an oscillating way with

time, so that dipoles will fluctuate too, they will radiate. When the particle size increases, or in other way, the wavelength diminishes, charges will create more complex charge distributions. In most of cases different resonant modes will be excited. This behavior can be observed in figures 1.2-1.3.

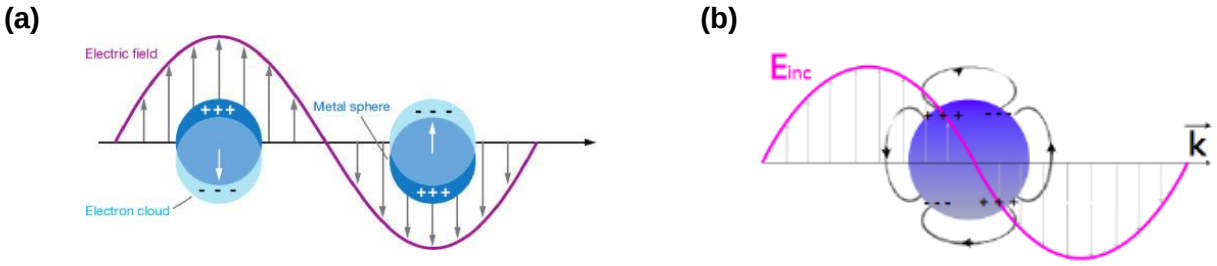

Figure 1.2: *(a) Particle is small comparing with the wavelength of incident field, a dipolar charge distribution is observed. (b) Particle size is bigger than in the previous case, so, charge distribution is quadrupolar.*

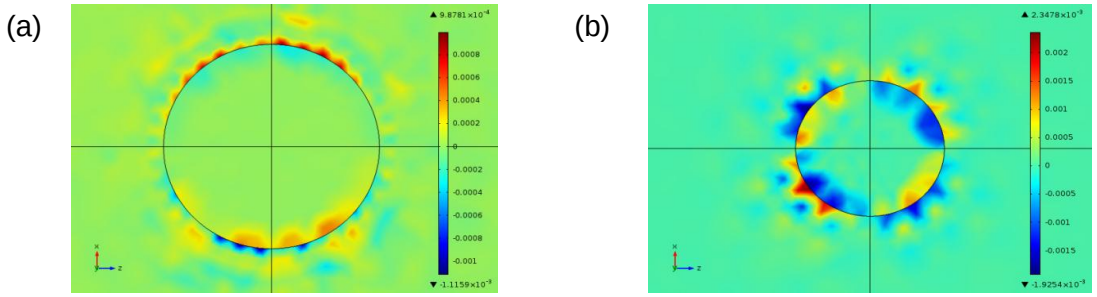

Figure 1.3: *Electric charge density of silver nanoparticles. The incident radiation corresponds to a plane wave polarized in x-axis and propagating in –z. (a) radius: 20nm, it is observed a dipolar charge distribution. The wavelength is: λ=360nm (b) radius: 70nm, we can see a quadrupolar charge distribution; λ=365nm.*

When electronic plasma is confined to very small regions, the magnitude order is of nanometers, electromagnetic energy is localized in smaller extensions than the wavelength of incident radiation and as a consequence an enhancement of the electric field is produced in vicinity of particle. These are called localized surface plasmons (LSP). In spite of this theory has been developed in the last century, gold nanoparticles were used in windows of cathedrals (figure 1.4) many years ago.

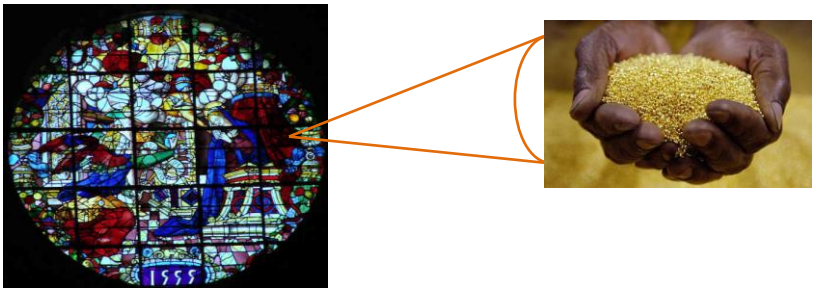

Figure 1.4: *The red color of windows is due to presence of gold nanoparticles in glass.*

Metals posses, as it will be commented in the section 5, a characteristic frequency, known as plasma frequency, which depends on electron density. This quantity is different for each metal and gives information about the limit frequency until which electron cloud is able to follow to incident field. If frequency of the wave corresponds to a certain frequency, resonance will be produced, so that energy radiation will be transferred to electrons and they will oscillate with maximum amplitude. Attending to particle size, optical constants and shape, resonance will be observed to different wavelengths, as it can be seen through the near field map obtained with COMSOL, see figure 1.5. This property is used for getting resonance to the appropriated wavelength for corresponding application.

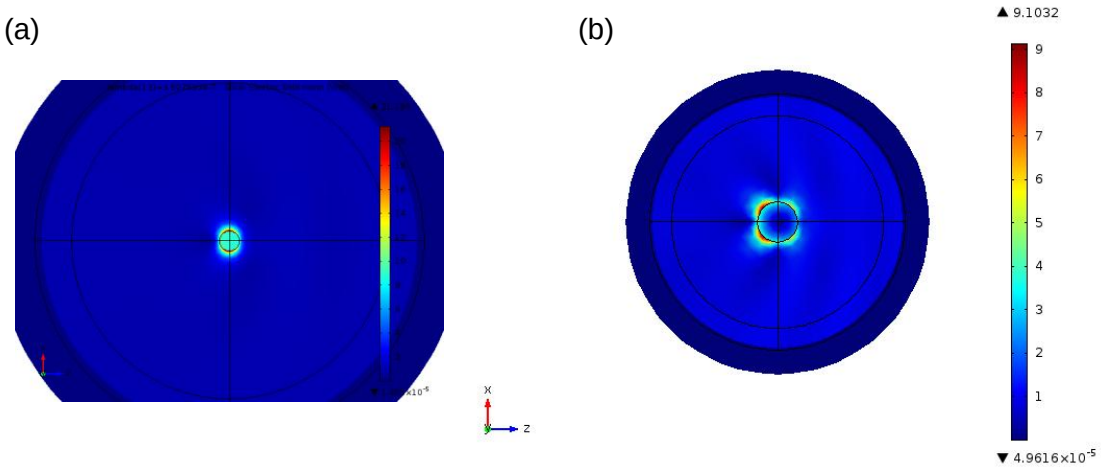

Figure 1.5: *Electric field norm. Particles are made of silver and in both cases they are illuminated by a plane wave polarized in x-axis and propagating in –z. (a) the radius of particle and the wavelength of incident wave are: r=20nm and λ=360nm respectively. (b)r=70nm and λ=365nm.*

Surface plasmons will be originated if the real part of dielectric constant is negative. With the objective of observing resonance properly, it is necessary condition that the imaginary part be small and positive, because this last term is associated with the Joule's losses. Materials that should be used in plasmonics must satisfy the following pair of conditions: [3]

$$\varepsilon_r < 0 \qquad \varepsilon_{im} << -\varepsilon_r$$

An example of material that verifies these two inequalities is silver. For this reason it has been chosen in this project.

2.1 Objectives

In the present work we have studied the electromagnetic interaction between two components of a dimer, when it is illuminated by an electromagnetic wave, as a function of inter-particle distance and their size. With the purpose of establishing differences between metallic and dielectric nanoparticles, we have chosen as materials silver and silicon. The study has been carried out paying attention to spectral properties, electric near field distribution and analysis of a spectral polarimetric parameter (linear polarization degree). We mostly focused on dipolar electric and magnetic resonances and in the linear polarization degree measured at 90º of the incident direction of light. Also, we study the influence in results of the geometric disposition of nanoparticles in space.

In order to achieve these goals, first of all we have studied the Mie theory, to know how light is scattered and absorbed by a small, spherical particle; Lorentz-Drude model, valid for metals, through it we can understand plasmon resonances that appear in spectra; the theory of "Whispering Gallery Modes", useful for dielectric particles with high refractive index; and the coupled dipole method, to study interaction between electric and magnetic dipoles. To calculate the corresponding parameters, we have used a numerical method that is able to solve the dimer problem. We have used COMSOL.

2.2 Work scheme

First of all, we have made a brief review of literature concerning to the topic of the project, which allows understanding the problem to solve. In the following pages are shown the main fundamentals of the different theories commented previously and the main nanoparticle applications. After that, results are shown with their analysis and conclusions that can be summarized of them. Initially, we have studied the Mie theory and created, by using Matlab, different programs that allow solving the problem of scattering and absorption of light by a small sphere. In a second step, we have revised the Drude model, the theory about "Whispering Gallery Modes", the coupled dipole method and different numerical methods, mostly COMSOL.

In the case of the metallic material, the following situations have been studied:

- Two identical particles, their radius were: 10*nm*
- Two identical particles, their radius were: 75*nm*

All the cases explained before have been repeated for the following gaps (inter-distance particles): 1, 10, 50, 100 and 200*nm* and for three different configurations: particles are located along the x-axis, y-axis and z-axis, and in all cases illuminated along z-axis. In the study of the dielectric particle, the size of dimer constituents has remained constant, with value: $r_1=r_2=150nm$. The gaps simulated were: 4, 10, 50, 100, 300*nm*. Again, we have studied the three different geometries, x-axis, y-axis, z-axis.

3.1 Absorption, scattering and extinction by a sphere

This theory was developed and published by Gustav Mie in 1908. From the Maxwell equations, and by a tedious mathematical development, he provided a physics explanation to the behavior of light absorbed and scattered by a small sphere.

It is known that for a linear, homogeneous and isotropic medium, the electromagnetic field must satisfy the following wave equations:

$$\nabla^2\vec{E}+k^2\vec{E}=0 \qquad \nabla^2\vec{H}+k^2\vec{H}=0 \tag{3.1}$$

where $\vec{E}$ and $\vec{H}$ are the electric and magnetic fields. *k* is given by: $k=\sqrt{\varepsilon\cdot\mu}\cdot\omega$, being *ε* and *μ* the electric permittivity and magnetic permeability of the medium respectively, and *ω* the angular frequency of radiation.

Considering that in a free charge medium, the divergence of electric and magnetic fields are null, $\nabla\vec{E}=0$, $\nabla\vec{H}=0$ and that both fields are related by the next expressions: $\nabla\times\vec{E}=i\omega\mu\vec{H}$; $\nabla\times\vec{H}=-i\omega\varepsilon\vec{E}$, it is built a vector function that verifies the wave equation and is divergence-free.

$$\vec{M}=\nabla\times(\vec{c}\psi) \tag{3.2}$$

where *ψ* is an scalar function and $\vec{c}$ is a vector constant.

In analogy to the relation between electric and magnetic fields, from the above expression, we are able to build another vector function, which also is divergence-free and accomplishes the wave equation:

$$\vec{N}=\frac{\nabla\times\vec{M}}{k} \tag{3.3}$$

$\vec{M}$ and $\vec{N}$ are named vector harmonics.

This pair of functions, 3.2-3.3, is analogous to that constituted by fields $\vec{E}$ and $\vec{H}$. By this way, the initial problem that involved solving the field equations has been simplified to an easier one, finding solution to the scalar wave equation ($\nabla^2\psi+k^2\psi=0$).

On account of geometry of particles, the scalar functions chosen for generating the vector harmonics, are functions that satisfy the wave equation in spherical polar coordinates:

$$\frac{1}{r^2}\frac{\partial}{\partial r}\left(r^2\frac{\partial\psi}{\partial r}\right)+\frac{1}{r^2\sin\theta}\frac{\partial}{\partial\theta}\left(\sin\theta\frac{\partial}{\partial\theta}\right)+\frac{1}{r^2\sin\theta}\frac{\partial^2\psi}{\partial\phi^2}+k^2\psi=0 \tag{3.4}$$

As it can be observed, this expression is a partial differential equation. With the objective of solving it, it is often used the separation of variables method, which yields to three differential equations.

$$\frac{d^2\Phi}{d\phi^2} + m^2\Phi = 0 \tag{3.5}$$

$$\frac{1}{\sin\theta}\frac{d}{d\theta}(\sin\theta\frac{d\Theta}{d\theta}) + [n\cdot(n+1) - \frac{m^2}{\sin^2\theta}]\Theta = 0 \tag{3.6}$$

$$\frac{d}{dr}(r^2\frac{dR}{dr}) + [k^2r^2 - n\cdot(n-1)]R = 0 \tag{3.7}$$

The solution to this group of equations corresponds with:

$$\psi_{emn} = \cos(m\cdot\phi)P_n^m(\cos\theta)z_n(k\cdot r) \tag{3.8}$$

$$\psi_{omn} = \sin(m\cdot\phi)P_n^m(\cos\theta)z_n(k\cdot r) \tag{3.9}$$

where *m* is an integer number, P_n^m are the associated Legendre functions of first kind of degree *n* and order *m*, where *n=m, m+1…* and z_n represents the spherical Bessel functions, that are related with the Bessel functions of first and second kind by the following way:

$$j_n(\rho) = \sqrt{\frac{\pi}{2\cdot\rho}}J_{n+\frac{1}{2}}(\rho) \tag{3.10}$$

$$y_n(\rho) = \sqrt{\frac{\pi}{2\cdot\rho}}Y_{n+\frac{1}{2}}(\rho) \tag{3.11}$$

where $\rho = kr$

The subscripts e (even) and o (odd) are concerned to the parity of solution corresponding to the function 3.5. The even solution is the cosine function and the odd one is the sine.

The outcomes are substituted in the expressions 3.2-3.3, obtaining the vector spherical harmonics, M_{emn}, N_{emn}, M_{omn}, N_{omn}, which are the normal modes of a spherical particle, transverse electric modes, (radial component of electric field is null), and transverse magnetic modes, (there is no radial magnetic field component). They are shown in the figure 3.1. [4]

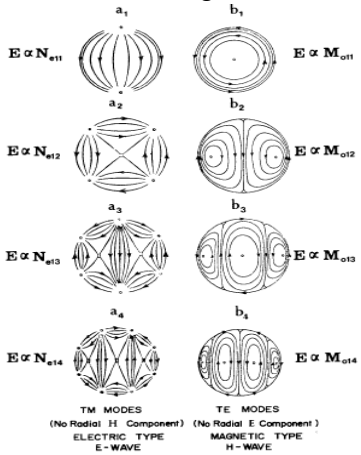

Figure 3.1: *Original scheme of the normal modes of the electric field, performed by Mie.*

The incident field, considered as a plane wave, is expressed as a linear combination of vector spherical harmonics:

$$\vec{E}_i = E_0 \sum_{n=1}^{\infty} i^n \frac{2 \cdot n + 1}{n \cdot (n+1)} (\vec{M}^{(1)}_{o1n} - i\vec{N}^{(1)}_{e1n}) \tag{3.12}$$

where the superscript (1) denotes that the Bessel functions that appear in the vector harmonics are of first kind.

Imposing the boundary conditions, the scattered field is determined.

$$\vec{E}_s = E_0 \sum_{n=1}^{\infty} i^n \frac{2 \cdot n + 1}{n \cdot (n+1)} (i a_n \vec{N}^{(3)}_{e1n} - b_n \vec{M}^{(3)}_{o1n}) \tag{3.13}$$

where the superscript (3) indicates that the z_n functions that appear in the vector harmonics are the Hankel functions, which are related with the spherical Bessel functions by the following way:

$$h_n^{(1)}(\rho) = j_n(\rho) + i \cdot y_n(\rho) \tag{3.14}$$

The coefficients that appear in the linear combination correspond to:

$$a_n = \frac{\mu \cdot m^2 \cdot j_n(m \cdot x)[x \cdot j_n(x)]' - \mu_1 \cdot j_n(x)[m \cdot x \cdot j_n(m \cdot x)]'}{\mu \cdot m^2 \cdot j_n(m \cdot x)[x \cdot h^{(1)}{}_n(x)]' - \mu_1 \cdot h^{(1)}{}_n(x)[m \cdot x \cdot j_n(m \cdot x)]'} \tag{3.15}$$

$$b_n = \frac{\mu_1 \cdot j_n(m \cdot x)[x \cdot j_n(x)]' - \mu \cdot j_n(x)[m \cdot x \cdot j_n(m \cdot x)]'}{\mu_1 \cdot j_n(m \cdot x)[x \cdot h^{(1)}{}_n(x)]' - \mu \cdot h^{(1)}{}_n(x)[m \cdot x \cdot j_n(m \cdot x)]'} \tag{3.16}$$

where μ and μ_1 are the magnetic permeability of the particles surrounding medium and of the particle, respectively. m is the relative refractive index and its expression is given by: $m=N_1/N$, being N_1 and N the refractive index of particle and surrounding medium.

As we can observe, in the argument of the spherical Bessel functions also appears the size parameter, which relates the size of particle with the refractive index of medium where it is immersed and with the wavelength of incident radiation, through the following equation:

$$x = \frac{2 \cdot \pi \cdot N \cdot a}{\lambda} \tag{3.17}$$

where a is the particle radius.

Similar equations to the scattered field can be found for the absorbed field, where the coefficients a_n and b_n are substituted by c_n

The number of terms of series that provides the values of absorbed and scattered fields, is infinity. In the performed study we have cut off the series in a determined n, which depends on the size of particle.

It is taken the nearest integer to the following operation:

$$x + 4 \cdot x^{1/3} + 2 \tag{3.18}$$

where *x* corresponds with the size parameter.

The cross sections are defined as areas whose dimensions are bigger than the particle are, because they are virtual surfaces that work like targets for incident radiation.

$$C_{sca} = \frac{2 \cdot \pi}{k^2} \sum_{n=1}^{\infty} (2 \cdot n + 1)(|a_n|^2 + |b_n|^2) \tag{3.19}$$

$$C_{ext} = \frac{2 \cdot \pi}{k^2} \sum_{n=1}^{\infty} (2 \cdot n + 1) \operatorname{Re}\{a_n + b_n\} \tag{3.20}$$

$$C_{abs} = C_{ext} - C_{sca} \tag{3.21}$$

Scattering, absorption and extinction efficiencies, Q, can be defined as the cross sections divided by the area of particle.

So, we obtain the following expressions:

$$Q_{sca} = \frac{C_{sca}}{\pi r^2} \qquad Q_{ext} = \frac{C_{ext}}{\pi r^2} \qquad Q_{abs} = \frac{C_{abs}}{\pi r^2} \tag{3.22}$$

3.2 Linear polarization degree

The incident field can be expressed as a function of the parallel and perpendicular components to the scattering plane, defined by directions of incident radiation propagation and scattering (figure 3.2).

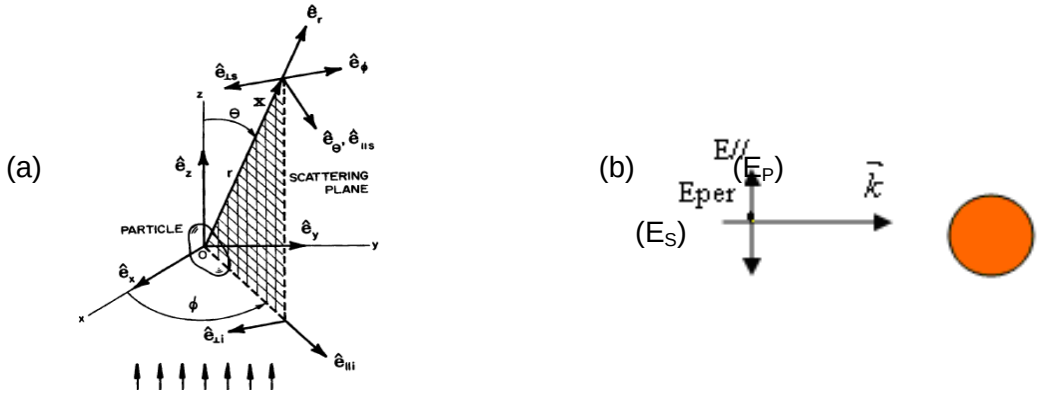

Figure 3.2: *(a) Light beam propagating in the z-axis and illuminating a particle. In the picture it is represented the scattering plane. (b) Scheme of the parallel (E_P) and perpendicular (E_S) to the scattering plane fields that illuminate the particle.*

The relation between scattered and incident fields can be expressed in a matrix way, through the Jones matrix that is characteristics of the system. In the Jones vectors, we write the parallel and perpendicular components to the scattering plane.

$$\begin{pmatrix} E_{pSca} \\ E_{sSca} \end{pmatrix} = \frac{e^{i\cdot k\cdot(r-z)}}{-i\cdot k\cdot r}\begin{pmatrix} S_2 & S_3 \\ S_4 & S_1 \end{pmatrix}\begin{pmatrix} E_{pInc} \\ E_{sInc} \end{pmatrix} \tag{3.23}$$

Another important representation is the scattering matrix, also known as Mueller matrix. The first one (Jones matrix) is only valid for systems in which scattered light is totally polarized. However, the scattering one is useful for beams that are partially polarized. Before defining the Mueller matrix it is necessary to define the Stoke's parameters. These correspond with the trace of resulting matrix of multiplying the identity matrix or one of Pauli´s matrices, with the polarization matrix (result of vectorial product of the Jones vector and its conjugate complex).

$$s_i = tr(\sigma_i \Phi) \tag{3.24}$$

where σ_i correspond with one of the following matrices:

$$\sigma_0 = \begin{pmatrix} 1 & 0 \\ 0 & 1 \end{pmatrix} \qquad \sigma_1 = \begin{pmatrix} 1 & 0 \\ 0 & -1 \end{pmatrix} \qquad \sigma_2 = \begin{pmatrix} 0 & 1 \\ 1 & 0 \end{pmatrix} \qquad \sigma_3 = \begin{pmatrix} 0 & -i \\ i & 0 \end{pmatrix} \tag{3.25}$$

and Φ is the polarization matrix, $\Phi = \varepsilon \times \varepsilon^{\dagger}$, being $\boldsymbol{\varepsilon}$ the Jones vector.

From the Stokes parameters, the definition of the Stokes vectors is immediate:

$$s = \begin{pmatrix} s_0 \\ s_1 \\ s_2 \\ s_3 \end{pmatrix} \tag{3.26}$$

The scattering matrix relates the Stokes vectors of scattered and incident fields. [5]

In the particular case that incident wave be linearly polarized, the Jones matrix is characterized for being diagonal:

$$\begin{pmatrix} E_{pSca} \\ E_{sSca} \end{pmatrix} = \frac{e^{i\cdot k\cdot(r-z)}}{-i\cdot k\cdot r}\begin{pmatrix} S_2 & 0 \\ 0 & S_1 \end{pmatrix}\begin{pmatrix} E_{pInc} \\ E_{sInc} \end{pmatrix} \tag{3.27}$$

where $S_1 = \sum_n \frac{2\cdot n+1}{n\cdot(n+1)}(a_n\cdot\pi_n + b_n\cdot\tau_n)$ and $S_2 = \sum_n \frac{2\cdot n+1}{n\cdot(n+1)}(a_n\cdot\tau_n + b_n\cdot\pi_n)$

The functions π_n y τ_n are known as angle-dependent and they are connected with the Legendre function of degree *n* and order 1 by the following expressions:

$$\pi_n = \frac{P_n^1}{\sin\theta} \qquad \tau_n = \frac{dP_n^1}{d\theta} \tag{3.28}$$

The linear degree of polarization is defined as:

$$P_L = \frac{i_s - i_p}{i_s + i_p} \tag{3.29}$$

where i_s and i_p correspond with scattered intensities perpendicular and parallel to the scattering plane, respectively. [6]

This parameter contains lot of information about the system. Through its study we get information about the charge distribution that is originating the resonance, the particle size, or in case of working with dimmers, the greater or lower interaction between particles that constitute it. Its range corresponds with the interval [-1, 1].

One of the most important measurements that is carried out frequently is the linear polarization degree at 90°, this implies measuring the scattered intensity at 90° respect to the propagation direction of incident light.

Substituting the values of i_s and i_p in the equation 3.27 and taking into account only the dipolar and quadrupolar terms of multipolar development of scattered field, which is a very good approximation in most of cases, we obtain an expression for the linear polarization degree that is easy to implement in a computer program.

$$P_L(90^o) = \frac{(9a_1 - 15b_2)^2 - (9b_1 - 15a_2)^2}{(9a_1 - 15b_2)^2 + (9b_1 - 15a_2)^2} \tag{3.30}$$

where a_1, a_2, b_1 and b_2, considering that the magnetic permeability of particle, $\mu = 1$ is the same as medium is, are given by:

$$a_1 = -\frac{i2x^3}{3}\frac{m^2-1}{m^2+2} - \frac{i2x^5}{5}\frac{(m^2-2)(m^2-1)}{(m^2+2)^2} + \frac{4x^6}{9}\left(\frac{m^2-1}{m^2+2}\right)^2 + O(x^7)$$

$$b_1 = -\frac{ix^5}{45}(m^2-1) + O(x^7)$$

$$a_2 = -\frac{ix^5}{15}\frac{m^2-1}{2m^2+3} + O(x^7) \tag{3.31}$$

$$b_2 = O(x^7)$$

In order to reach part of the objectives of this work and get conclusions, we have established some approximations:

- If electric and magnetic quadrupolar terms are negligible, the equation 3.27 will be simplify to the following expression, which is valid when the particles behave like dipoles:

$$P_L(90^o) = \frac{|a_1|^2 - |b_1|^2}{|a_1|^2 + |b_1|^2} \tag{3.32}$$

We can see that when the value of P_L is positive ($P_L>0$) will predominate electric dipolar effects, otherwise, ($P_L<0$), the magnetic dipolar effects dominate over the electric ones.

- Considering that magnetic effects do not contribute, b_1 and b_2,

P_L is reduced to:

$$P_L(90^o) = \frac{9|a_1|^2 - 25|a_2|^2}{9|a_1|^2 + 25|a_2|^2} \tag{3.33}$$

A positive result means that charge distribution is predominantly dipolar, but, in the other case, it is mostly quadrupolar.

Intensity pattern emitted by an electric dipole is a very interesting representation in electromagnetism.

In the far field approximation, distance from origin to point where is calculated the electric field is much bigger than wavelength of exciting radiation, ($kr >> 1$), for an unpolarized beam, we obtain the following expression of scattered intensity by an electric dipole:

$$I_s = \frac{8\pi^4 N a^6}{\lambda^4 r^2}\left|\frac{m^2-1}{m^2+2}\right|(1+\cos^2\theta)I_i \qquad (4.1)$$

This equation can be discomposed in two different ones, one of them corresponding to situation in which incident radiation is parallel to the scattering plane, and the other one referred to the perpendicular case, obtaining:

$$i_p = \frac{9|a_1|^2}{4k^2r^2}\cos^2\theta \qquad i_s = \frac{9|a_1|^2}{4k^2r^2} \qquad (4.2)$$

We have created a program by using Matlab that allows plotting in polar coordinates the scattered intensity for the three situations aforementioned. The results obtained are shown in the figure 4.1. [4]

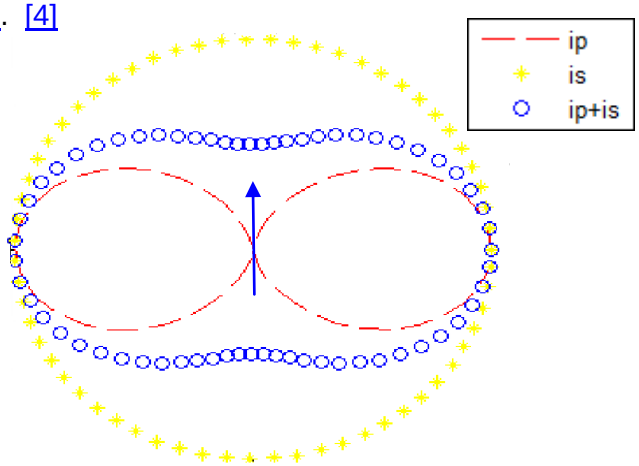

Figure 4.1: *Scattered intensity by a sphere with a dipolar electric charge distribution in the following cases: incident radiation is perpendicular to the scattering plane, exciting wave is parallel to the scattering plane, and the incident beam is unpolarized. The arrow represents the electric dipole.*

As we can observe in the figure, intensity patterns are symmetric, which is consistent with the geometry of problem, spherical particle.

We also can see that in case of studying a small particle, comparing with the wavelength of exciting radiation, and illuminate it with linearly polarized light, parallel to the scattering plane, it is obtained as intensity pattern an inverted eight that radiates in

transversal direction to the electric dipole. So that, if we measure the scattered intensity at 90°, we obtain value zero. However, if initial polarization is perpendicular to the scattering plane, angular distribution of scattered light is a circle, so, in any point of the scattering plane where we measure intensity, we will obtain the same value. Considering this assumption, the linear polarization degree corresponds to 1, which is a coherent conclusion, because we are working with an electric dipolar charge distribution.

If we are far from the dipolar electric behavior, the intensity pattern loses the eight-shape, subsequently, the P_L measured at 90° is lower than 1. This value is a consequence of the greater contribution of parallel intensity.

If we consider a particle where the most important effects are magnetic ones, being the electric negligible, the image that we find is opposite to the figure 4.1. This means that, when particle is illuminated with light polarized parallel to the scattering plane, the pattern is a circle, and when incident radiation is perpendicular to that plane, the figure is an inverted eight (see figure 4.2). So that, P_L value corresponding to a magnetic dipolar charge distribution is equal to -1.

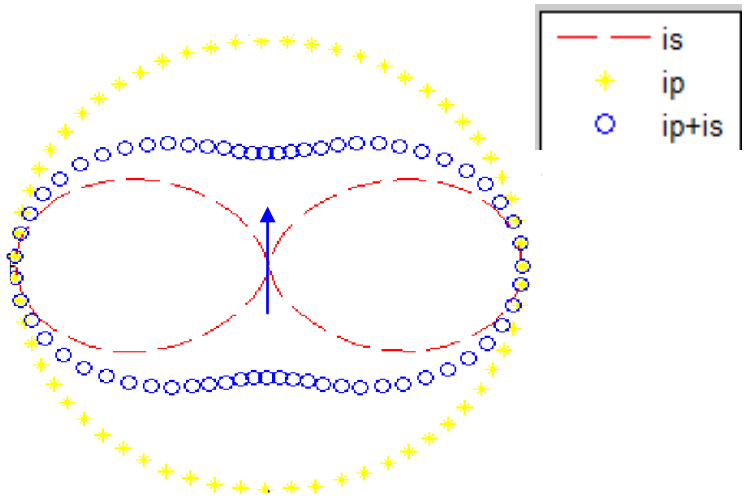

Figure 4.2: *Representation of the scattered intensity by a sphere with a magnetic dipolar charge distribution, in the following situations: incident radiation is parallel to the scattering plane, it is perpendicular to it, it is unpolarized.*

5.1 Drude-Lorentz model

Lorentz postulated in 1878 that matter was constituted by electric dipoles. Each one of them characterized by its resonance frequency. When electromagnetic radiation illuminates matter, dipoles start to oscillate, emitting radiation.

The Drude model dates back to 1900. According to this model, inside atoms we can distinguish two different parts: the "cores" that are constituted by the core of the atom, as we conceive it nowadays, and deeper electrons, and the conduction electrons, which are delocalized between cores, and are considered like punctual particles that move freely in a box (figure 5.1). For studying free electrons we have to use the kinetic theory of gases. It is able to explain the electrical and thermal conductivity. The incorporation of this theory to the Lorentz model is known as the Drude-Lorentz model.

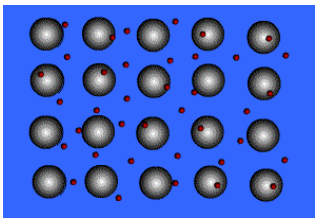

Figure 5.1: *Representation of the cores (positively charged), in grey color and the delocalized electrons between cores (negatively charged), in red.*

An electric dipole is a system of two charges of opposite sing but of the same magnitude. The dipole moment is giving by:

$$\vec{P} = q\vec{d} \tag{5.1}$$

where *q* corresponds with electric charge and $\vec{d}$ is the vector that joins the charges, as it is observed in the figure 5.2.

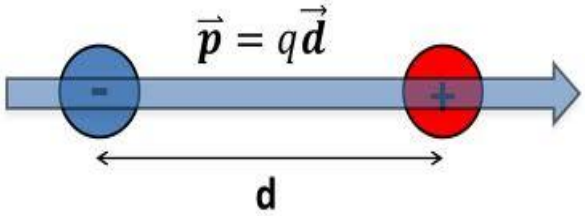

Figure 5.2: *Dipole moment.*

Attraction between cores charged positively and bound electrons, negatively, can be modeled in a mechanical way by introduction of an inelastic oscillator (figure 5.3).

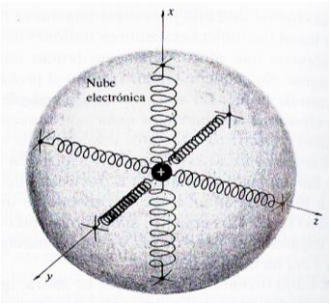

Figure 5.3: *Interaction between a core and bound electrons in the Drude-Lorentz model.*

Due to the presence of an external electric field, charge distribution is disturbed, so that, matter acquires a certain polarization, which comes from the following expression:

$$\vec{P} = \varepsilon_0(\chi_E - 1)\vec{E} \tag{5.2}$$

where ε_0 and χ_E correspond to the vacuum permittivity and electric susceptibility respectively.

Considering only the bound electrons we can make the following reasoning:

From arguments of classical mechanics, it is considered that the displaced electron cloud experiments a restoring strength that is proportional to displacement. If the direction of electric field is *x* it is obtained the following expression:

$$F = -kx \tag{5.3}$$

where the restoring constant, *k*, is related with the natural frequency of dipole through the electron mass.

$$k = \omega_0{}^2 m_e \tag{5.4}$$

Electron mass should be substitute by reduced mass of system, μ:

$$\frac{1}{\mu} = \frac{1}{m_e} + \frac{1}{m_N} \tag{5.5}$$

m_N corresponds with the core mass. [7]

However, using m_e we obtain basically the same results.

Considering the second Newton's law, it can be described the dynamic of system. It is a forced oscillator:

$$m_e\ddot{x} = -kx + q_e E_0 e^{i\omega t} \tag{5.6}$$

being m_e and q_e the mass and charge of the electron respectively.

The solution to the differential equation 5.6 is:

$$x(t) = \frac{q_e}{(\omega_0{}^2 - \omega^2)m_e} E(t) \tag{5.7}$$

So that, the dipole moment can be describe as:

$$P(t) = q_e x(t) N = \frac{q_e{}^2 N}{m_e(\omega_0{}^2 - \omega^2)} E(t) \tag{5.8}$$

N corresponds to electron density.

The resonant frequency is different for each one of dipoles that constitute the atom, so, it is necessary to modify a little bit the above equation:

$$P(t) = \frac{q_e{}^2 N}{m_e} \sum_i \frac{f_i}{(\omega_0)_i{}^2 - \omega^2} E(t) \tag{5.9}$$

where f_i is the oscillator strength.

We must consider a dissipative term because of charge is oscillating. It behaves as a radiating dipole.

$$m\ddot{x} = -kx - \gamma m\dot{x} + q_e E_0 e^{i\omega t} \tag{5.10}$$

γ is the damping constant. Solving the equation 5.10 we find that polarization is given by:

$$P(t) = \frac{q_e{}^2 N}{m_e} \sum_i \frac{f_i}{(\omega_0)_i{}^2 - \omega^2 + i\gamma_i\omega} E(t) \tag{5.11}$$

However, in a metal it is possible to differentiate bound and free electrons. In the Lorentz model the behavior of bound electrons is correctly described by using oscillators, but, free electrons do not possess a natural frequency, so that, we have to add another term in the equation 5.10 that takes them into account.

$$P(t) = \frac{q_e{}^2 N}{m_e} \left[\frac{f_e}{-\omega^2 + i\gamma_e\omega} + \sum_i \frac{f_i}{(\omega_0)_i{}^2 - \omega^2 + i\gamma_i\omega} \right] E(t) \tag{5.12}$$

Free electrons (ω_0=0)

f_e and γ_e are oscillator strength and damping constant of free electrons respectively.

Beginning with the equation 5.12 can be extracted the following conclusions:

- If the frequency of incident radiation is far of the resonance frequency, free electrons term will be dominant.

- In the case of high frequencies, $\omega^2 >> \omega\gamma_e$, polarization will be determined by the following equation:

$$P(t) = -\frac{q_e{}^2 N}{m_e \omega^2} E(t) = -\left(\frac{\omega_P}{\omega}\right)^2 \varepsilon_0 E(t) \tag{5.13}$$

being ω_P the plasma frequency: $\omega_p = \left(\frac{N \cdot q_e{}^2}{\varepsilon_0 \cdot m_e}\right)^{1/2}$ (5.14)

From the equation 5.13 it is immediate to express the refractive index as a function of the plasma frequency and distinguish two different cases:

$$n^2(\omega) = 1 - \left(\frac{\omega_p}{\omega}\right)^2 \tag{5.15}$$

- $\omega<\omega_p$, refractive index is a complex number, particles absorb most of the radiation, however, the electromagnetic radiation does not propagate inside metal.

- $\omega>\omega_p$, refractive index is a real number, it is produced the inverse situation with respect to the aforementioned case, waves propagate without being absorbed.

5.2 Resonance frequency for the electric dipole

In the simplest case, particle behaves as an electric dipole, we can deduce the frequency at which resonance will be found, and as a consequence, a big enhancement of the field will be produce in the surrounding of particle. Due to charge redistribution that takes place when electromagnetic wave illuminates the particle, it is caused a polarization in the particle that is proportional to external electric field.

$$\vec{P} = \varepsilon_0 \alpha \vec{E} \tag{5.16}$$

The constant α is related with the electric permittivity of particle:

$$\alpha = \frac{3 \cdot d^3}{4 \cdot \pi} \frac{\varepsilon - \varepsilon_0}{\varepsilon + 2\varepsilon_0} \tag{5.17}$$

Clausius Mossotti relation

where *d* is the radius of particle, ε and ε_0 are the electric permittivities of the particle and vacuum respectively.

Through the expressions 5.16-5.17 we can observe that as ε tends to the value $-2\varepsilon_0$, greater is the mentioned constant, α, and consequently, polarization. With the objective of knowing frequency which we have to illuminate the particle with, in order to produce the greater polarization, we must impose the relation between electric permittivity and plasma frequency:

$$\frac{\varepsilon}{\varepsilon_0} = 1 - \frac{\omega_p^{\ 2}}{\omega^2} \Rightarrow \omega = \sqrt{\frac{\varepsilon_0 \omega_p^{\ 2}}{\varepsilon_0 - \varepsilon}} \tag{5.18}$$

As it was said before, polarization presents a maximum when ε takes a value near to $-2\varepsilon_0$. Substituting this condition in the equation 5.18 we find that for getting maximum oscillating amplitude, frequency of incident wave should be related with plasma frequency as follows:

$$\omega = \frac{\omega_p}{\sqrt{3}}$$

The interaction of electromagnetic waves with matter exhibits a different behavior depending on material which is made of the particle, metallic or dielectric. The main observed differences, are the outcome of two factors: optical constants and free electrons. In metallic materials, the electric permittivity is a complex number and there are free electrons, nevertheless, in the dielectric case, it is real and in the conduction band free electrons are not found.

The complex part of refractive index is responsible for the absorption, as it was explained in the Drude-Lorentz model. For this reason, Joule`s losses are not so important in dielectric materials as in metallic ones.

Owing to the absence of free electrons, in dielectric materials, plasmonics resonances are not observed, and another similar phenomenon takes place, it is known as whispering gallery modes. The effect produced is the same that occurs in cathedrals where we consider sound travelling along the domes. A whispering emitted in a part of dome can be heard in some specific places where constructive interference in produced. [7]

In addition to electric resonances, in the dielectric materials can also appear magnetic resonances [8], as we can observe in the near field map showed in the figure 6.1, as a consequence of the field propagation inside the particle. The magnetic response is originated by displacement currents. The recent interest in studying the dielectrics with high refractive index is based on their multiple applications.

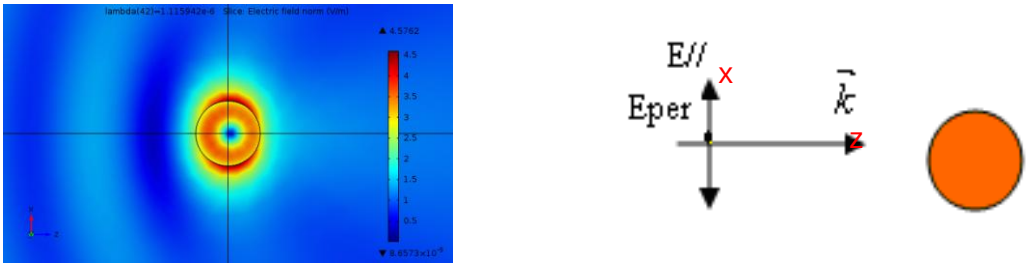

Figure 6.1: *Representation of the electric field norm for a Silicon nanoparticle, whose radius is 150nm, when it is illuminated with an electromagnetic wave, λ=1116nm, polarized in x-axis, propagating in z-axis. On the right of this figure it is observed the description of the scattering geometry.*

Due to one of the objectives of this work is to understand the electromagnetic behavior of dimmers illuminated by an electromagnetic wave, in the following section we are going to consider the interaction between dipoles, electric and magnetic. It is obvious that interaction will be a function of distance. The greater is distance, the lower is interaction.

Electric and magnetic fields generated by an electric dipole are determined by the following expressions:

$$\vec{E}_P = \frac{1}{4\pi\varepsilon_m\varepsilon_0}[\vec{p}\frac{e^{ikr}}{r}(k^2 - \frac{1}{r^2} + \frac{ik}{r}) + \vec{n}(\vec{n}\cdot\vec{p})\frac{e^{ikr}}{r}(-k^2 + \frac{3}{r^2} - \frac{3ik}{r})] \quad (7.1)$$

$$\vec{H}_P = \frac{1}{4\pi\sqrt{\mu_m\mu_0\varepsilon_m\varepsilon_0}}[(\vec{n}\times\vec{p})\frac{e^{ikr}}{r}(k^2 + \frac{ik}{r})] \quad (7.2)$$

These equations are valid to calculate the electric and magnetic fields in any point of space to a distance r and direction $\vec{n}$ from the dipole, being ε_m and μ_m the electric permittivity and magnetic permeability relative to medium surrounding the particles. [9]

In the animated gif below is shown the electric field emitted by an electric dipole.

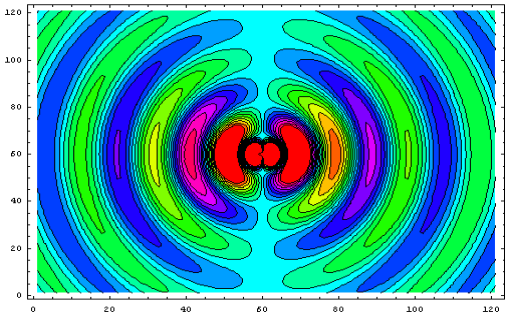

Figure 7.1: *Electric field emitted by an electric dipole.*

These last expressions can be simplified for two extreme situations, near field and far field.

In the far field approximation, (*kr>>1*), the most important contribution is supported by terms that contain 1/r. For this reason the equations 7.1-7.2 are reduced to the following expressions:

$$\vec{E}^{ff}{}_P \approx k^2\frac{e^{ikr}}{4\pi\varepsilon_m\varepsilon_0 r}[\vec{p} - \vec{n}(\vec{n}\cdot\vec{p})] \qquad \vec{H}^{ff}{}_P \approx k^2\frac{e^{ikr}}{4\pi r\sqrt{\mu_m\mu_0\varepsilon_m\varepsilon_0}}(\vec{n}\times\vec{p}) \quad (7.3)$$

For obtaining near field expressions, we must take the limit when $kr << 1$, in the electrostatic limit: [10]

$$\vec{E}^{nf}{}_{P} \approx \frac{1}{4\pi\varepsilon_m\varepsilon_0 r^3}[3\vec{n}(\vec{n}\cdot\vec{p})-\vec{p}] \qquad \vec{H}^{nf}{}_{P} \approx ik\frac{1}{4\pi r^2}\sqrt{\mu_m\mu_0\varepsilon_m\varepsilon_0}(\vec{n}\times\vec{p}) \quad (7.4)$$

In analogy, electric and magnetic fields created by a magnetic dipole are given as follows [9]:

$$\vec{E}_m = -\frac{1}{4\pi}\sqrt{\frac{\mu_m\mu_0}{\varepsilon_m\varepsilon_0}}(\vec{n}\times\vec{m})\frac{e^{ikr}}{r}(k^2+\frac{ik}{r}) \quad (7.5)$$

$$\vec{H}_m = \frac{1}{4\pi}[\vec{m}\frac{e^{ikr}}{r}(k^2-\frac{1}{r^2}+\frac{ik}{r})+\vec{n}(\vec{n}\cdot\vec{m})\frac{e^{ikr}}{r}(-k^2+\frac{3}{r^2}-\frac{3ik}{r})] \quad (7.6)$$

Making the corresponding approximations for near and far field we get these expressions [10]:

$$\vec{E}^{ff}{}_{M} \approx -k^2\sqrt{\frac{\mu_m\mu_0}{\varepsilon_m\varepsilon_0}}\frac{e^{ikr}}{4\pi r}(\vec{n}\times\vec{m}) \quad \vec{H}^{ff}{}_{M} \approx k^2\frac{e^{ikr}}{4\pi r}[\vec{m}-\vec{n}(\vec{n}\cdot\vec{m})] \quad (7.7)$$

$$\vec{E}^{nf}{}_{M} \approx -ik\sqrt{\frac{\mu_m\mu_0}{\varepsilon_m\varepsilon_0}}\frac{1}{4\pi r^2}(\vec{n}\times\vec{m}) \quad \vec{H}^{nf}{}_{M} \approx \frac{1}{4\pi r^3}[3\vec{n}(\vec{n}\cdot\vec{m})-\vec{m}] \quad (7.8)$$

where $\vec{m}$ is the magnetization, which is related with magnetic field: $\vec{m} = \chi\vec{H}$, being χ the magnetic susceptibility.

Known the expressions of the electric and magnetic fields created by an electric or magnetic dipole, it is convenient to analyze two important configurations: longitudinal and transverse, (see figure 7.2), for knowing aspects related with their interaction.

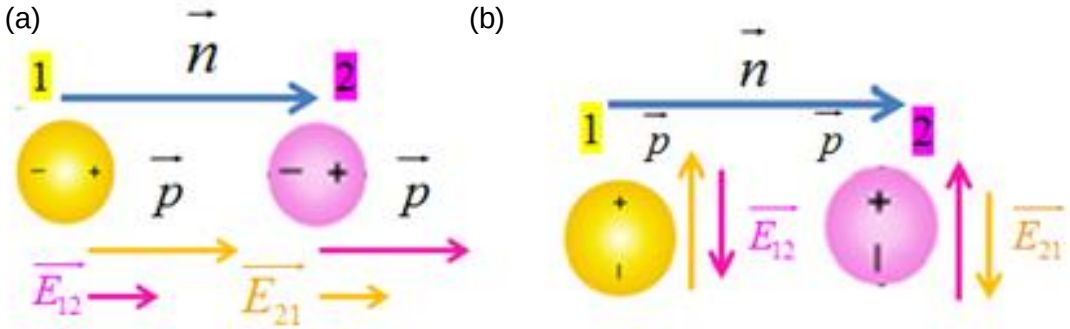

Figure 7.2: *Interaction between two electric dipoles. a) Longitudinal configuration. b) Transverse configuration.* $\vec{n}$ *is the unitary vector in the direction that joins both of particles,* $\vec{p}$ *is the polarization in the particles originated by the incident electric field and* $\vec{E}_{12}$ *and* $\vec{E}_{21}$ *are the fields created in the particle 1 by the particle 2 and in the particle 2 by the particle 1 respectively.*

We have considered two identical particles, small comparing with wavelength of incident radiation, that present a dipolar charge distribution. In near field approximation:

Longitudinal configuration

Polarization of both particles is in the same axis that line which joins their centers. Electric field created in particle 2 by particle number 1 has the same modulus and direction as the field created by particle 2 in particle 1, both of them present the same direction as polarization created in the particle as a consequence of the incident field. The interaction strengthens initial polarization. Taking into account the geometry of problem, the dot product, $\vec{n}\cdot\vec{p}$, corresponds to the *p* modulus, the angle between this pair of vectors is zero. So that the expression 7.4 left, can be write as:

$$\overrightarrow{E_{12}} = \overrightarrow{E_{21}} \approx \frac{\vec{p}}{2\pi\varepsilon_m\varepsilon_0 r^3} \qquad (7.9)$$

a) Transverse configuration:

Polarization of particles is orthogonal to line that joins the center of both of them. Electric field that creates particle 1 in 2 is of the same modulus as the field created in particle 2 by 1, and they are placed in the same direction. However, the direction of fields is opposite to polarization originated by the incident field, so, it is produced a weakening of initial polarization. In this case, the dot product is zero, because the angle formed between the vectors $\vec{n}$ and $\vec{p}$ is 90º.

$$\overrightarrow{E_{12}} = \overrightarrow{E_{21}} \approx -\frac{\vec{p}}{4\pi\varepsilon_m\varepsilon_0 r^3} \qquad (7.10)$$

In addition, comparing the two different configurations, equations 7.9-7.10, it is easy to prove that, in modulus, the field produced in longitudinal situation is twice that produced by the dipoles in the another studied configuration.

If we are in the far field approximation, in longitudinal configuration, the electric field that a dipole creates in the axis that joins both particles is zero, however, in transversal configuration, the field produced in dipole 2 by dipole 1 is the same as the generated in dipole 1 by 2 and both of them present the direction of the initial polarization. This field strengthens the polarization of each one of particles, as we can see through the next equation:

$$\overrightarrow{E}^{ff}{}_P \approx k^2 \frac{e^{ikr}}{4\pi\varepsilon_m\varepsilon_0 r}\vec{p} \qquad (7.11)$$

In first approach, each one of components of the dimer, suffers the presence of two fields: incidence and that produced by the dipolar charge distribution of its partner. Once again, the total field generated in the particles will create a field in the other constituent of system, and this process will be repeated until a stationary situation is gotten. Due to the interaction, we can see an enhancement of the field in the gap that separates them.

In order to obtain conclusions for magnetic dipoles, it can be followed the same reasoning carried out for the electric ones.

In a two spherical particles problem, due to interaction between them, it is not possible to use the Mie theory and solve it analytically. Because of that, we have to resort to numerical methods. Some of the most important are: point-matching method [11], the discrete dipole approximation [11], T-matrix [12], the finite element method [13], COMSOL. The last one was the method that we used in the project.

COMSOL:

It is based on finite element method. It is characterized for being a program that allows solving partial differential equations in an efficient way, for that cause, it is interesting in electromagnetism and in other contexts of physics and engineering.

In the electromagnetism module, it is possible to build the desired geometry for the considered problem, defining number of particles and their position. Also, you can choose material which particles and surrounding medium are made of and introduce the kind of wave with its polarization and propagation direction (Figure 8.2).

In the mesh, it is usually used tetrahedral as we can observe in figure 8.1, number of selected elements must be enough to get precise results. Its graphic interface is very nice for visualizing the absorbed and scattered fields in near field, the absorption, scattering and extinction cross sections, and the far field in 2-D and 3-D. Attending to symmetry of problem: geometric and physics, some simplifications are made.

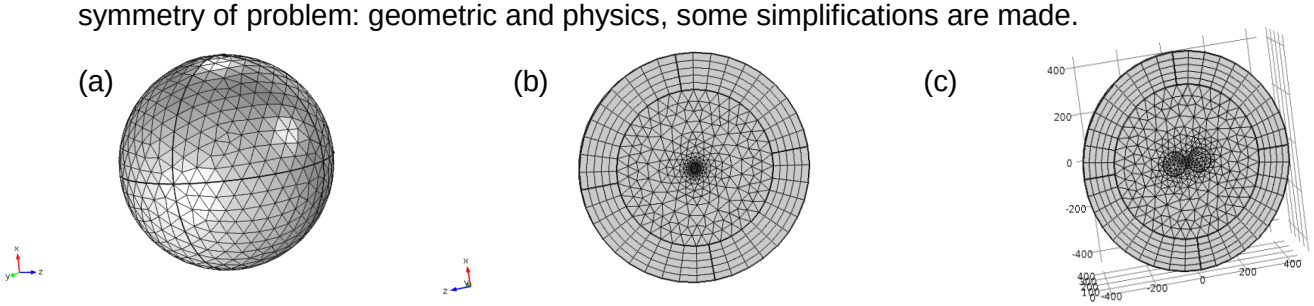

Figure 8.1: *(a) We can observe the tetrahedra chosen for the mesh. (b) Cutting the sphere. We have assumed that incident wave is propagating in z-axis and is polarized in x-axis. Magnetic field is symmetric respect to y-axis (perfect magnetic conductor). (c) Cutting the sphere for a dimer.*

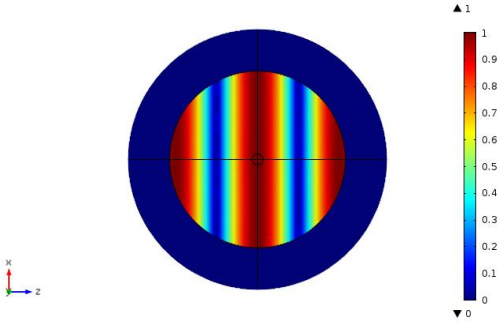

Figure 8.2: *Incident electric field. It corresponds with a plane wave polarized in x-axis and propagating in z-axis.*

Nanotechnology has revolutionized science of last decades. Possibility of manipulating matter to nanometric scale, has generated advantages in such different fields like: medicine, pharmacology, intelligent materials, environment…

Nowadays it is possible to carry out some ideas that only existed in science fiction. One example is the film "Viaje alucinante", in which is related the travel of some scientifics, who reduce their size to a particle and introduce themselves into body of an investigator in order to destroying the tumor that is killing him. In a similar argument is based the film: "Cariño he encogido a los niños", in this movie it is thought about reducing things by laser.

Plasmon resonances that take place in metallic nanoparticles, are characterized for three different properties: quality factor, Q_F, oscillator strength, f and modal volume, V_m. [14]

Quality factor is a measurement of amplitude enhancement of the local field when particle is excited by a resonant wavelength. Also, it gives information about number of oscillations that a surface plasmon undergoes before it decays. This parameter is related with the optics properties of particles by the following equation:

$$Q_F = -\frac{\mathrm{Re}(\varepsilon)}{\mathrm{Im}(\varepsilon)} \tag{9.1}$$

For noble metals, as gold and silver, the value of this magnitude ranges between 10-100. Taking into account that the intensity enhancement is proportional to Q_F^2, the increase produced is proportional to 10^2-10^4. From these results we can observe as metallic nanoparticles present a high value of quality factor.

The oscillator strength corresponds to number of electrons in the conduction band. Absorption cross section is proportional to f, whereas the scattering one is to f^2. The cross sections are until 10 times greater than the particle real area.

The modal volume is the nanoscopic volume in which the plasmon is localized. In the case of small particles this magnitude corresponds with real particle volume, for this reason, a confinement of the optical energy is produced.

All the commented characteristics make to metallic nanoparticles interesting in multiple applications like solar cells, medical treatments, transport of drugs…

9.1 Medicine and pharmacology

In this field, it is very important biochips manufacturing. From them, scientific get genetic information that allows creating vaccines, measuring resistance of tuberculosis strains to antibiotics, or identifying mutations that some genes experiment and that play a role in tumor illnesses, like is the case of gen P-53 in the breast and colon cancers.

It has been possible to improve detection of viral particles, studying localized plasmon resonance in different metallic nanoparticles. With gold nanoparticles, some proofs for combating flu have been done.

In the case of silver nanoparticles, due to their antibacterial activity, they are used as coatings on certain implants or in healing of burns. In fact lots of prostheses are covered of this kind of nanoparticles. [15]

9.1.1 Cancer treatment

Metallic nanoparticles can be used for cancer treatment through a thermal phototerapy. They are constituted by a dielectric core and a gold shell (figure 9.1). These particles present resonances in the near-infrared range. When they are introduced into body, they link to cancerous cells; a bit amount of nanoparticles adhere to healthy ones. Performance is based on illuminating the system with resonant radiation, so that, absorption phenomena takes place. This process is more important than scattering due to small size of particles. Thanks to Joule effect, heating is produced, which kills pathogenic cells, unchanging the healthy ones. [16]

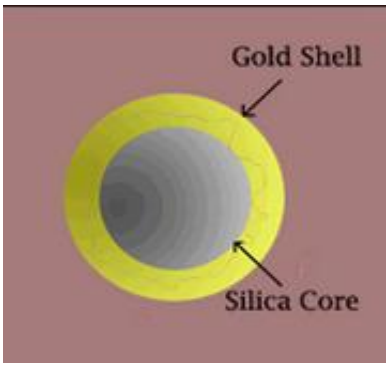

Figure 9.1: *Nanoparticle made of a silicon core and a gold shell.*

With respect to pharmacology, nanodrugs that liberate medicine from inside of cells, deserve special mention. These systems act like drug carriers. Their main advantages are: degradation ease and diffusion through the biological barriers, allowing access to target cells. There are some nanodrugs that serve as cancer treatment; one of them consists on using gold nanoparticles as it is shown in the figure below.

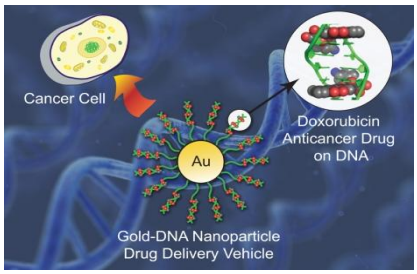

Figure 9.2: *Scheme of performance of a gold nanoparticle as drug carrier.*

9.2 Solar cells

Renewable energy, in spite of its profits, is not used frequently by two main reasons: it is expensive and its efficiency is low. Metallic nanoparticles have been implemented in solar cells for concentrating light in an efficient way.

With development of nanophotonics, three different configurations have been studied for improving efficiency of solar cells (figure 9.3). [16]

a) Due to the scattering properties of nanoparticles, incident sunlight is trapped in Si semiconductor.
b) In the resonance wavelength, interaction between electromagnetic radiation and matter is very important, so that an enhancement of the electric field is produced in surrounding of nanoparticles, which are close to the semiconductor. Because of absorption is proportional to electric field intensity, an amplification of it will be produced to the resonance frequency.
c) Nanoparticles couple the incident light into a guide mode in the semiconductor, which propagates until it is completely absorbed.

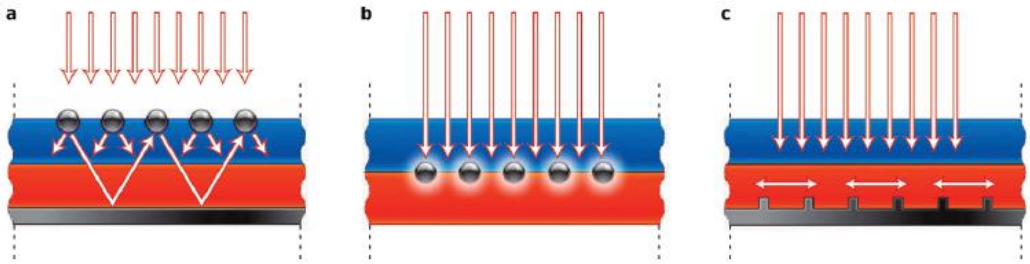

***Figure 9.3**: The most common configurations in solar cells. a) Light is trapped in the semiconductor due to scattering phenomenon. b) It is produced strong absorption to resonance frequency. c) Light is coupled to a guide mode. [16]*

9.3 Surface-Enhanced Raman Scattering

It is a spectroscopy technique based on the Raman Effect. It consists on vibrational spectrum amplification of molecules that are settled onto nanostructured metallic surface. It is used for detecting biologic materials, which present strong absorption in a concret electromagnetic range, in low concentrations. [16]

The recent interest in generating sensors for detecting different substances, has promoted development of this technique. Some of the most important applications are: detection of drugs, environment pollution, and control of food.

A practice example is the study carried out in U.S.A for combating the terrorist attaches suffered in 2011 using anthrax. The SERS tags consist on gold nanoparticles covered by Silicon (figure 9.4). These SERS targets are linked to an antibodie and they produce a strong spectroscopic signal. From this method it is possible to confirm or reject

presence of the analyte. Molecules conjugated to antibodies capture and concentrate the SERS-labeled complex in focal point of a laser. [17]

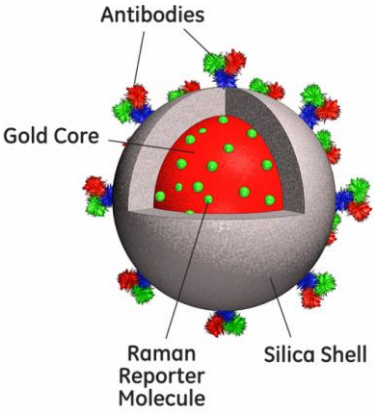

Figure 9.4: *Scheme of the nanoparticle studied in 2011 for combating terrorist attaches.*

9.4 Intelligent materials

The intelligent materials are those derived of nanotechnology, whose properties can be changed and controlled as we want. These materials are able to change their colors, forms, electronic properties, as a consequence of different inputs (light, sound, temperature or voltage). The possibility of creating components with atomic precision allows building materials with high electrical conductivity.

Metamaterials:

The physical properties of each one of components are different to those of whole material. These materials do not exist in nature, impressive properties are caused by structural design. Components must be smaller than wavelength of incident radiation.

These materials present a negative refractive index and the Poynting vector points in opposite sense to propagation direction.

One of the most important applications is manufacturing of flat lenses, which are able to focusing light in smaller areas than incident wavelength. This technology could be implemented in optics computers that would be quicker than the actual ones, although their development has not advanced too much.

9.5 Dielectric nanoparticles

We have commented the main applications of metallic nanoparticles, but we have not said anything about the dielectric ones. However, the fact that they do not present energy losses makes them interesting as alternative to metallic particles.

In this sense, as we will see, nanospherical dielectric particles with high refractive index, depending on their size and shape, exhibit defined electric and magnetic resonances in different electromagnetic ranges. Another interesting property is the directionality. Adjusting particle size and wavelength of incident radiation, in the case of

silicon, we can observe that scattered intensity in the forward-direction is six times greater than in backward-direction. Considering Kerker conditions, [18], [19], [20] light can be only scattered in forward or backward direction.

Because of these properties, this kind of materials is very attractive for manufacturing different devices like nanoantennas (figure 9.5) [21], nano-waveguides, or nanolenses.

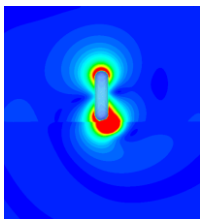

Figure 9.5: *Local field of a single emitter coupled to an antenna.*

In the section 10.1 we analyze the cases of metallic isolated particles in order to familiarize with different concepts studied in the theory and understand the performance of COMSOL. We have chosen three particles sizes corresponding to r=20, 50, 70*nm*.

In the section 10.2 we present the results for a metallic dimer, silver. We have simulated two different particle sizes, r=10, 75*nm*. For these two sizes we have studied the following gaps: 200, 100, 50, 10, 1*nm*.

In the section 10.3 we have showed the results for a dielectric dimer, silicon. In this case the size of components have remained constant r=150*nm*. The gaps studied correspond to: 300, 100, 50, 10, 4*nm*.

For all the cases we have analyzed the spectral efficiency plots, near field maps and the spectral linear polarization degree measured at 90º, $P_L(90º)$. Also, for the metallic dimer we have simulated the norm of electric field in the center of gap.

10.1 Isolated metallic particles

We have compared obtained results with COMSOL and Matlab. We have analyzed three isolated particles of radius: r=20*nm*, r=50*nm* and r=70*nm*. In all cases, particles are embedded in air and incident light is polarized in x-axis and propagates in –z-axis (see figure 10.1), where we represent the analyzed geometry. Amplitude of incident electric field is E_0=1.

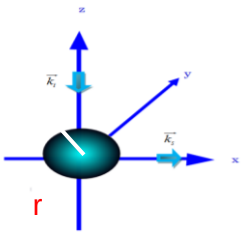

Figure 10.1: *Description of scattering geometry. The scattering plane is z-x.*

In figure 10.2 we represent a comparison of the results obtained with the program that we have developed and with COMSOL. We have plotted the values of the efficiencies and Mie coefficients: a_1, a_2, b_1 and b_2 for different sizes.

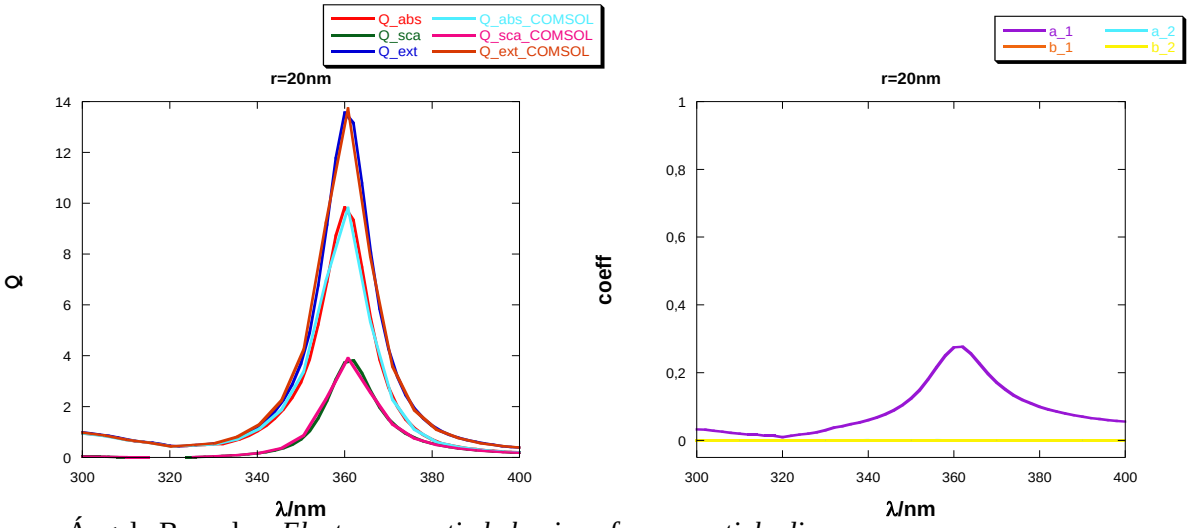

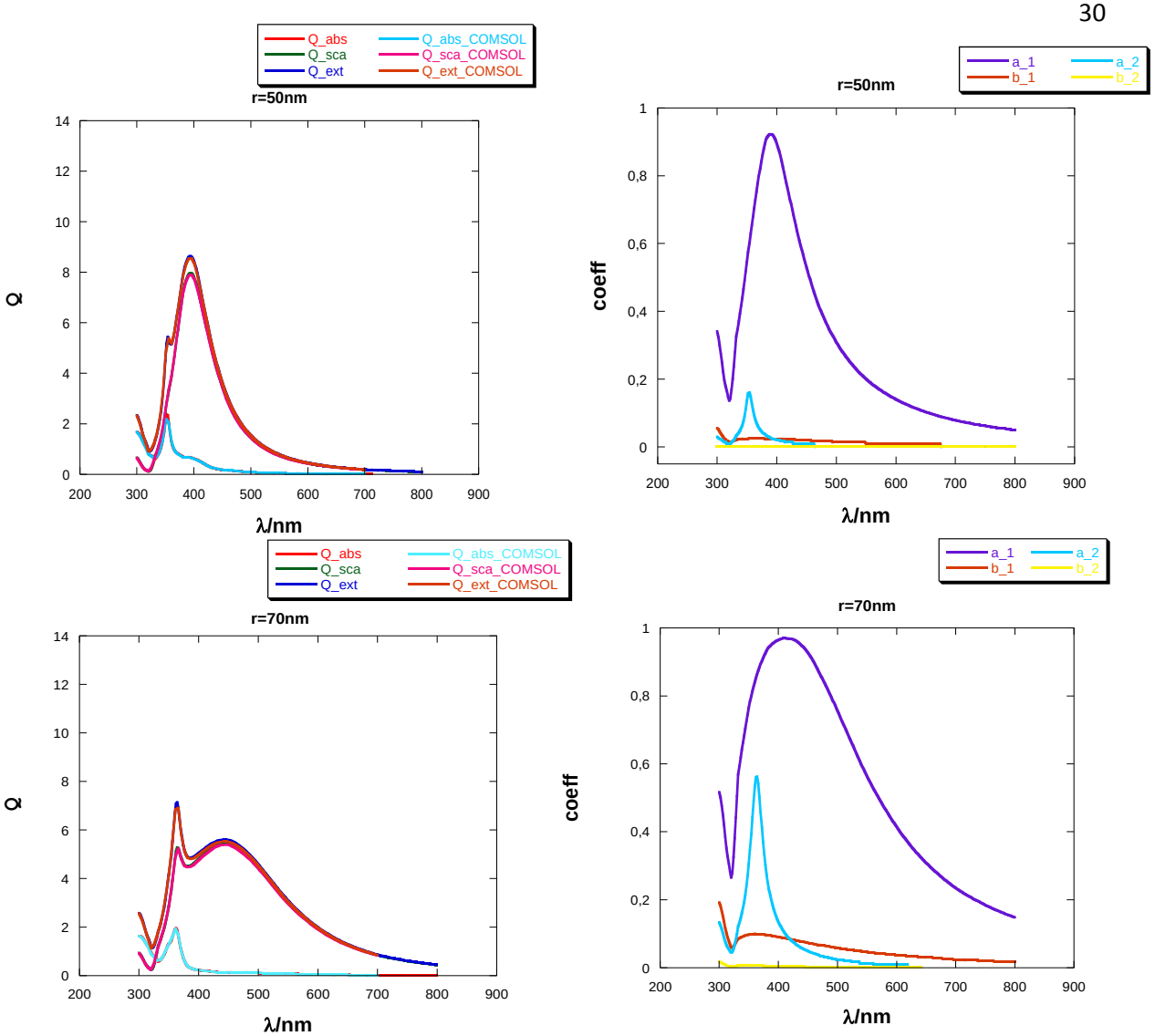

Figure 10.2: *On left colum it is represented absorption, scattering and extinction efficiencies obtained with COMSOL and with Matlab program. On the right, Mie coefficients, a_1, a_2, b_1 and b_2, are shown for the three chosen particle sizes.*

As can be seen, the adjustment of obtained results with both methods is almost perfect.

In the case of a small particle, whose radius is: 20*nm*, it is observed only a peak in the spectrum corresponding to an electric dipolar resonance and the only contribution to the extinction efficiency (see eq. 3.20) is given by the term a_1.

For the particle of radius r=50*nm* appears a new peak due to an electric quadrupolar resonance. The term a_2 becomes important.

In the last analyzed case, r=70*nm*, we can observe the same peaks as in plot corresponding to r=50*nm*. However, the quadrupolar term takes more importance than the dipolar one. Also, b_1 coefficient, magnetic dipolar effect, starts to appear.

Through obtained results, we can observe that as particle size increases, new resonances of high order will appear. So that, not only the dipolar electric contributions are present, a_1, but the electric quadrupolar, a_2, are too. Also, resonances broaden and a red-shift of dipolar peaks is produced. In case of small particles, extinction efficiency

is given by absorption. However, for bigger particles the extinction is mainly due to scattering of light.

We have also studied the spectral behavior of the linear polarization degree at 90°, $P_L(90º)$. The observation was in x-axis, see (figure 10.3):

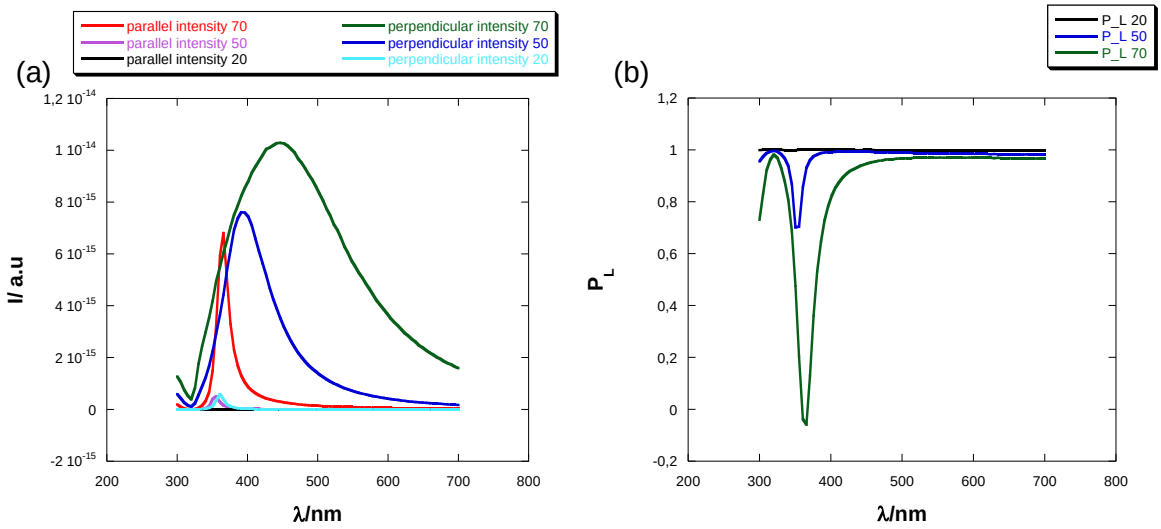

Figure 10.3: *(a) Parallel and perpendicular to the scattering plane, z-x, intensities. (b) P_L measured at 90º (x-axis) for the three sizes studied.*

In case of a particle with a radius corresponding to r=20*nm* the value of the P_L is one. Because of the particle behaves as an electric dipole. As the particle size increases, the P_L decreases, reaching, in case of r=70*nm*, negative results, due to the presence of quadrupolar and magnetic effects (b_1 takes significant values).

Finally in (figure 10.4) we represent the electric scattered field norm in the near field region for a silver particle of radius 50*nm* obtained with COMSOL and the program that we developed. We observe an enhancement in the vicinity of the particle. The results are very similar in both analyzed cases.

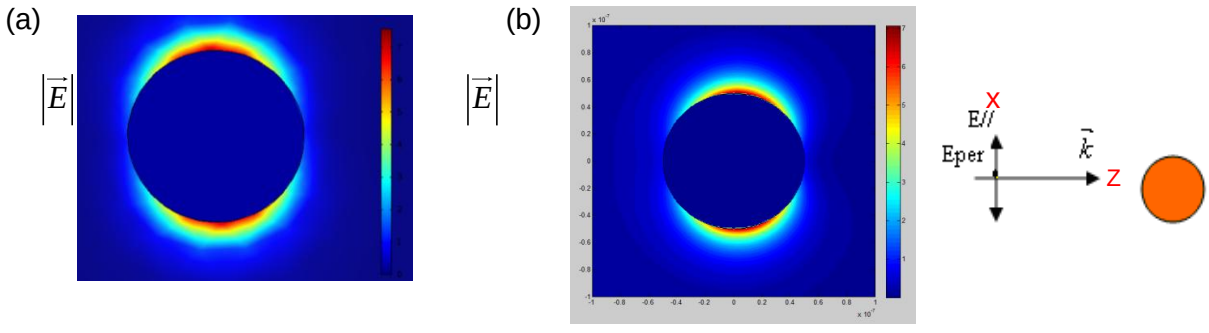

Figure 10.4: *Electric scattered field norm in near field region. The particle was illuminated with a plane wave whose wavelength is λ=406nm, corresponding to the electric dipolar resonance. (a) Image obtained with COMSOL. (b) Image obtained from Matlab program.*

10.2 Metallic dimer: Silver

It has been studied interaction between two identical silver particles, for different gaps. System has been illuminated with a plane wave propagating in –z-axis, for two different polarizations: in x-axis and in y-axis. Amplitude of the incident electric field was supposed E_0=1 (a.u), see figure 10.5.

We have analyzed three different geometries. Because of brevity we have only shown the results corresponding to x-axis case. Nevertheless, at the end of this analysis we have made the timely comments for the other configurations.

Particles in x-axis **Particles in y-axis** **Particles in z-axis**

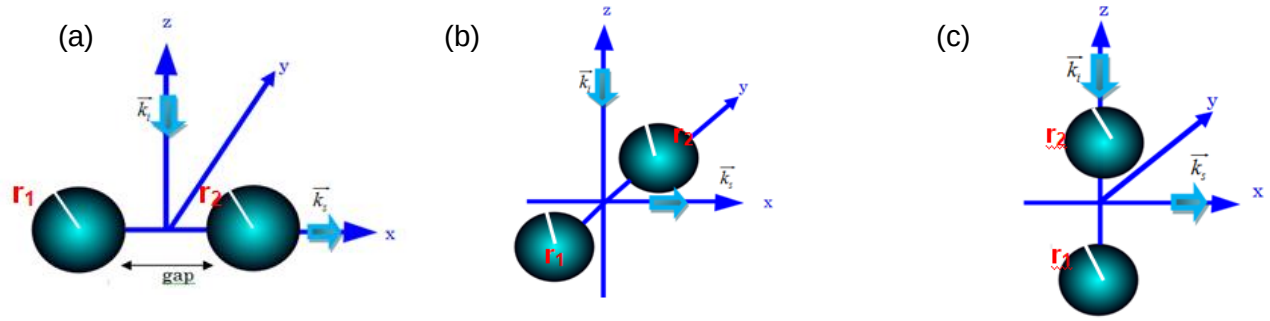

Figure 10.5: *Description of scattering geometry. The scattering plane is z-x. (a) particles in x-axis, (b) in y-axis, (c) in z-axis.*

Particles in x-axis

- **r_1=10*nm* r_2=10*nm***

In order to know interaction between the components of dimer, we should compare the obtained results with case of an isolated particle, so that, it is the first plot that we present, (see figure 10.6).

Isolated particle:

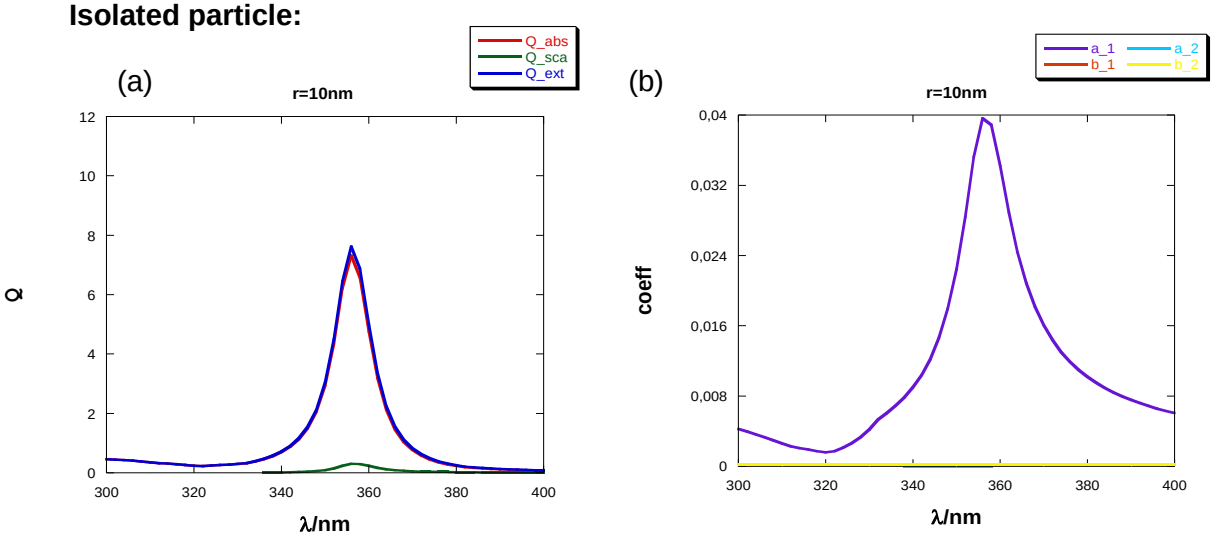

Figure 10.6: *(a) Efficiency plots for an isolated particle of radius 10nm. (b) Coefficients a_1, a_2, b_1, b_2.*

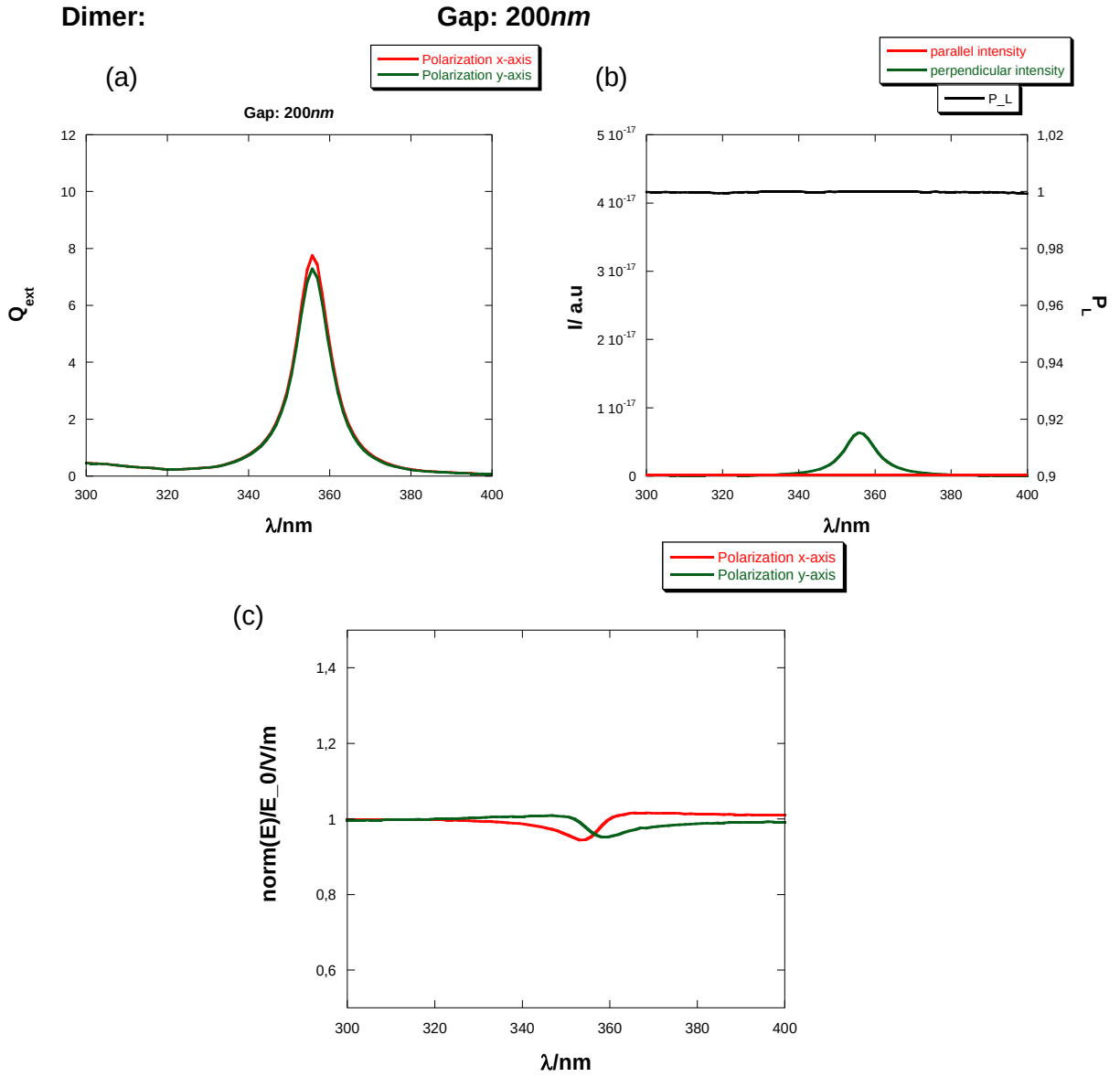

Figure 10.7: *(a) Extinction efficiencies. (b) Parallel and perpendicular intensities and $P_L(90º)$. (c) Norm of electric field in the center of gap.*

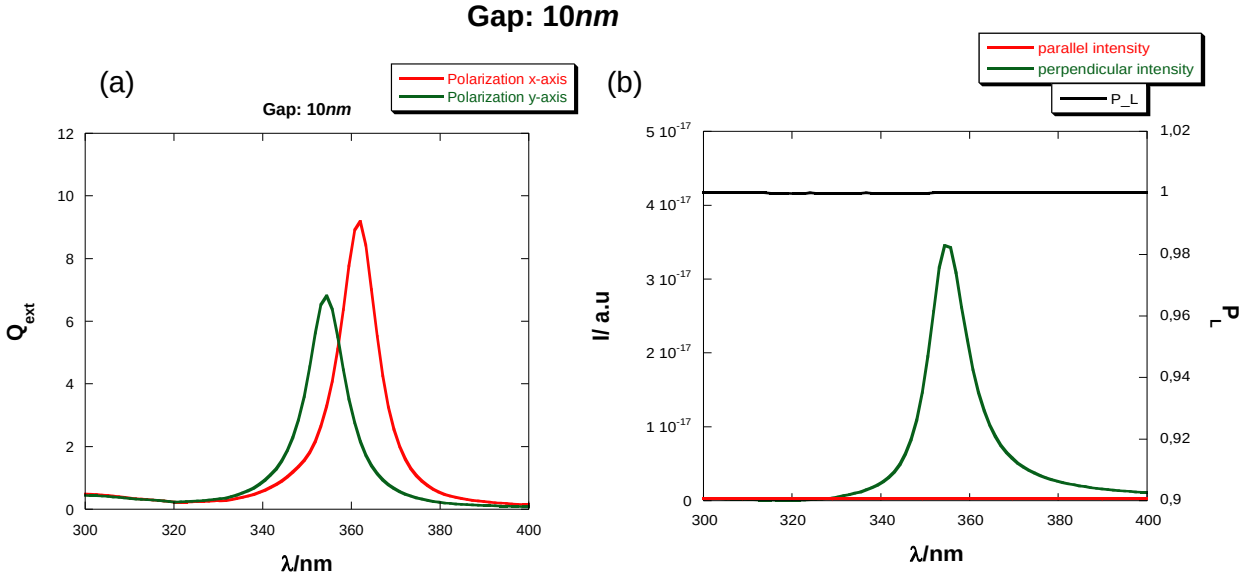

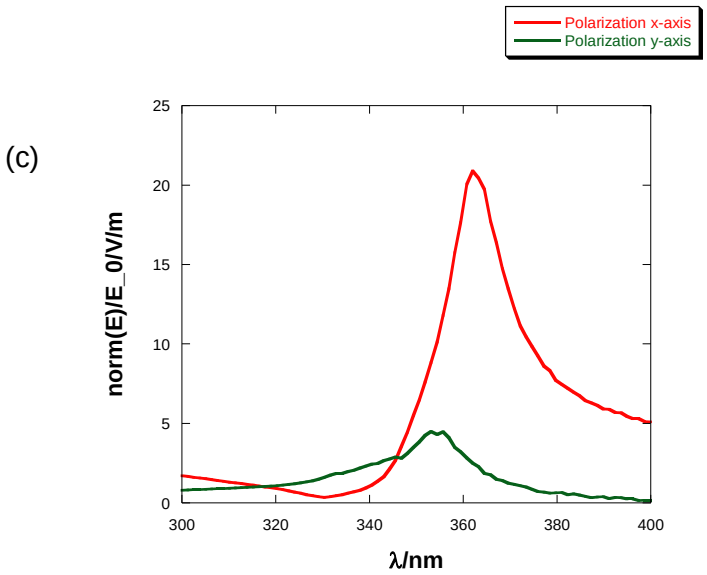

Figure 10.8: *(a) Extinction efficiencies. (b) Parallel and perpendicular intensities and $P_L(90º)$. (c) Norm of electric field in the center of gap.*

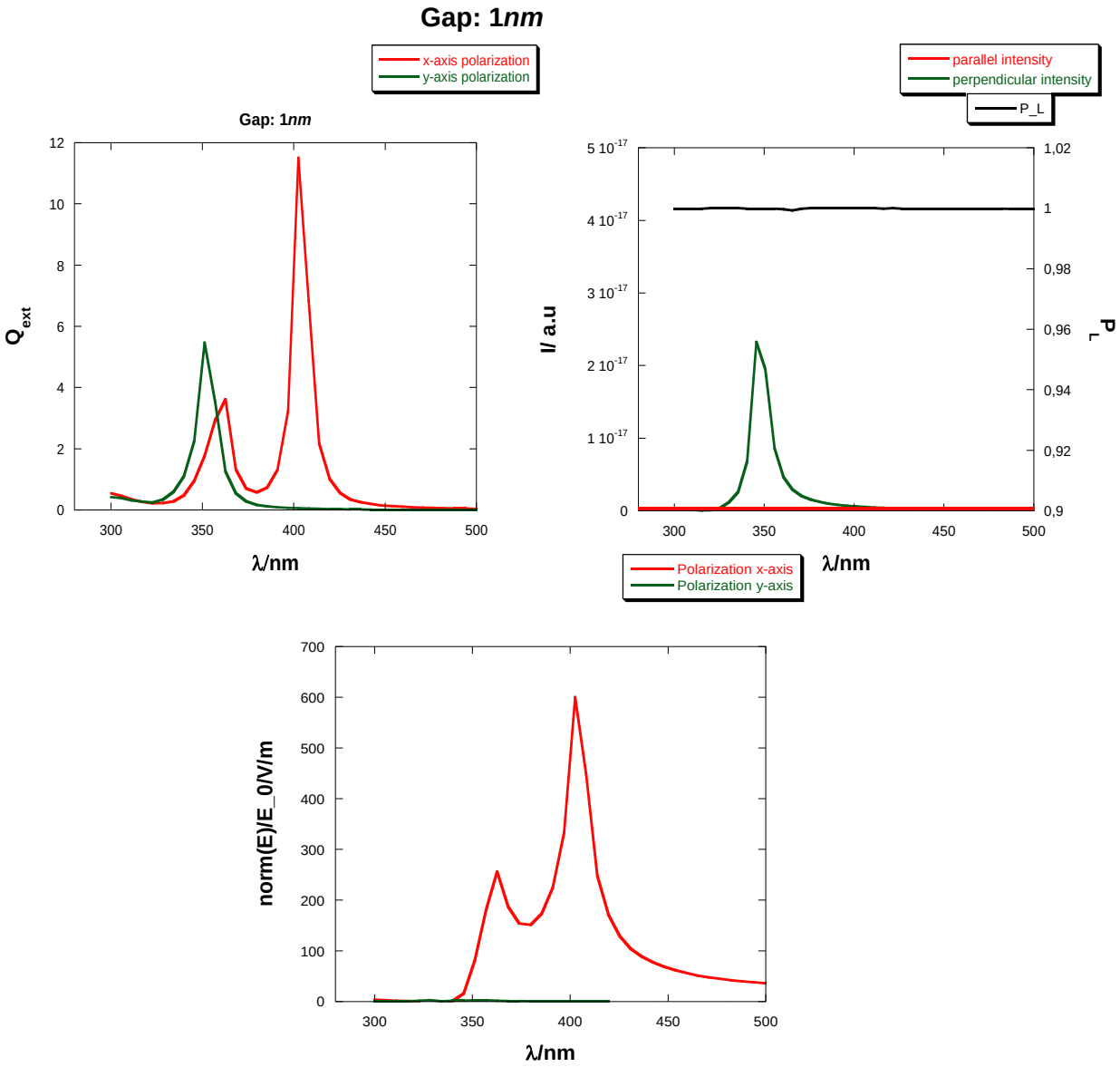

Figure 10.9: *(a) Extinction efficiencies. (b) Parallel and perpendicular intensities and $P_L(90º)$. (c) Norm of electric field in the center of gap.*

The results obtained for gaps corresponding to 100 and 50*nm* are the same as for 200*nm* are. For that reason we have only represented one of them.

In cases corresponding to gaps: 200, 100 and 50*nm* and longitudinal configuration, see figure 7.2, absorption, scattering and extinction efficiencies are the same as in case of an isolated particle. This means that particles do not interact each other, because of the gap is much larger than their sizes. Dimer cross sections are twice those for the isolated one. In the intensity plot it is only observed perpendicular contribution, this agrees with the obtained value of $P_L(90°)$, 1, and with fact that charge distribution corresponds to a dipole. Extinction efficiency plots for transversal configuration are similar to the latter case. However, in this configuration, in far field, interaction is significant, and the height of the resonance peak increases with respect to the isolated particle. The electric field norm in the center of gap takes a value nearly to one. This means that electromagnetic interaction between particles is negligible.

When particles get closer, interaction becomes important. In the two cases that are going to be analyzed, gap=10, 1*nm* near field approximation can be considered, eq 7.7 and 7.8.

In the case corresponding to 10*nm* gap, we observe different extinction efficiency plots depending on polarization of the incident light. For polarization in x-axis, longitudinal configuration, it is represented an increase in Q_{ext}, due to electromagnetic interaction between both particles. In longitudinal configuration, dipoles emit along the line that links their centers, (x-axis), this emission strengthens the polarization of particles. Also, a red-shift is shown with respect to the isolated particle. However, in transversal configuration, polarization in y-axis, we can see a blue-shift, accompanied with a decrease of efficiency. Because of interaction, it is created in each one of particles an electric field that is opposed to incident one. Observed spectral shifts can be explained by the "toy model", see figure 10.10. In the case of an isolated particle, due to presence of an electric field, it is produced a redistribution of electric charges along its surface, these charges suffer "repulsive forces". When another particle is included in the system, and incident field is parallel to the direction that joins both components, a weakening of that force is produced, and as a consequence we find a decrease of frequency. In transversal configuration, repulsive force increases and because of that, oscillator strength does it too.

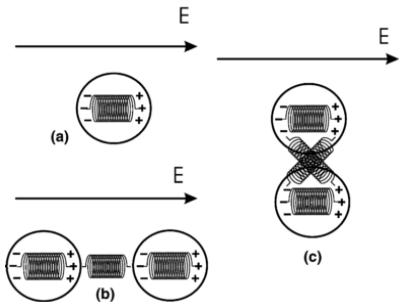

Figure 10.10: *(a) Isolated particle. (b) Longitudinal configuration, it is produced a weakness of repulsive force between surface charges. (c) Transversal configuration, repulsive force increases.* *[22]*

Trough the P_L analysis we can conclude that charge distribution corresponds to an electric dipole, P_L "don`t see" the interaction. By the results of $|\vec{E}|$ in the gap center, we observe that electric field value has suffered an enhancement because of interaction.

In the case corresponding to 1*nm* gap, in longitudinal configuration, plots show a red-shift and an increase of efficiencies. Also, a new peak is observed. It appears to lower wavelengths than the corresponding with dipolar resonance. This is due to hybridization phenomena. In the other configuration, height of maximum decreases with respect to above case, gap 10*nm*, produced by a greater interaction between particles. Looking at the P_L graph, we also can conclude that charge distribution is a dipole, P_L "see" all the system like a dipole. Through the modulus of the electric field plot in center of gap, it is shown an important enhancement due to particles are very close each other and the interaction is very strong.

With respect to hybridization, as particles separation diminishes, interaction between a determined *l* mode of a particle and higher *l* modes of the other component of dimer is produced. *[23]*

In figure 10.11 we show near field maps for two different gaps: 200 and 1*nm* for longitudinal configuration. When particles are very close each other, 1*nm*, a hot spot can be observed.

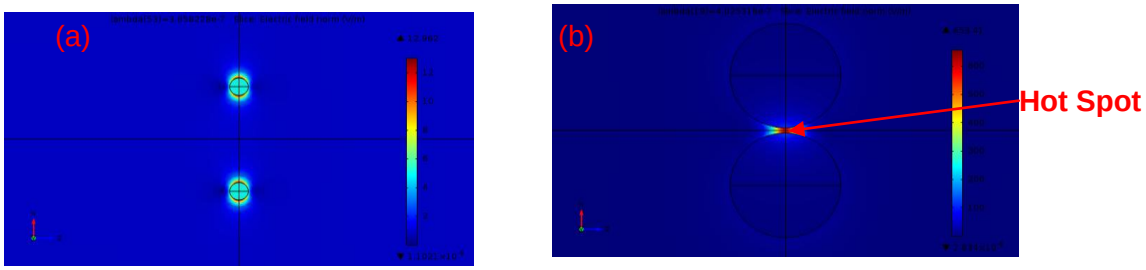

Figure 10.11: *Electric field norm for a silver dimer, r_1=10nm r_2=10nm, when it is illuminated by a plane wave, polarized in x-axis and propagating in –z-axis. (a) gap:100nm, wavelength λ=366nm. (b) gap: 1nm, λ=400nm.*

- **r_1=75*nm* r_2=75*nm***

Isolated particle:

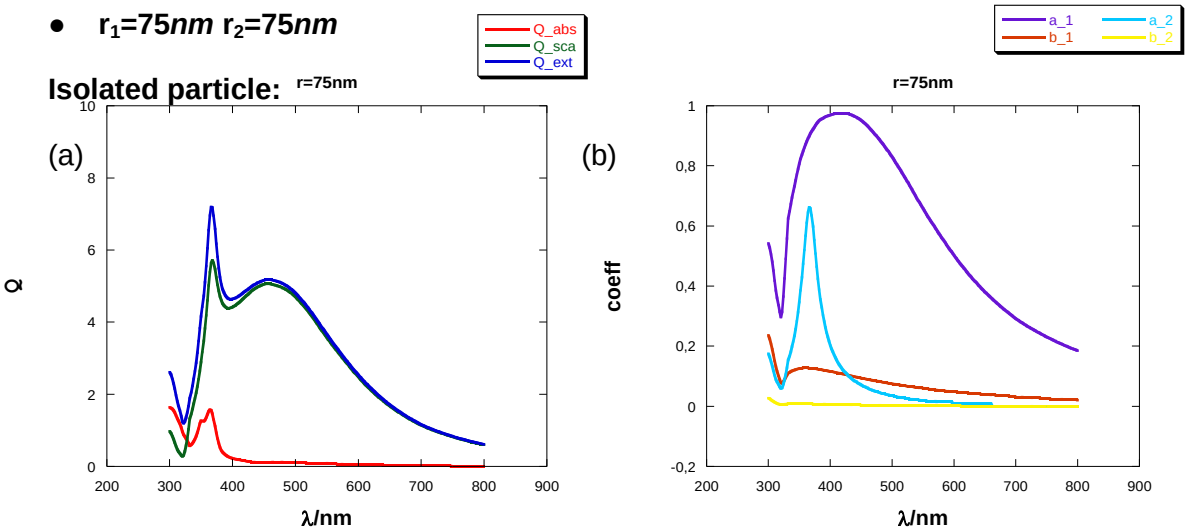

Figure 10.12: *(a) Efficiency plots for an isolated particle of radius 75nm. (b) Coefficients a_1, a_2, b_1, b_2.*

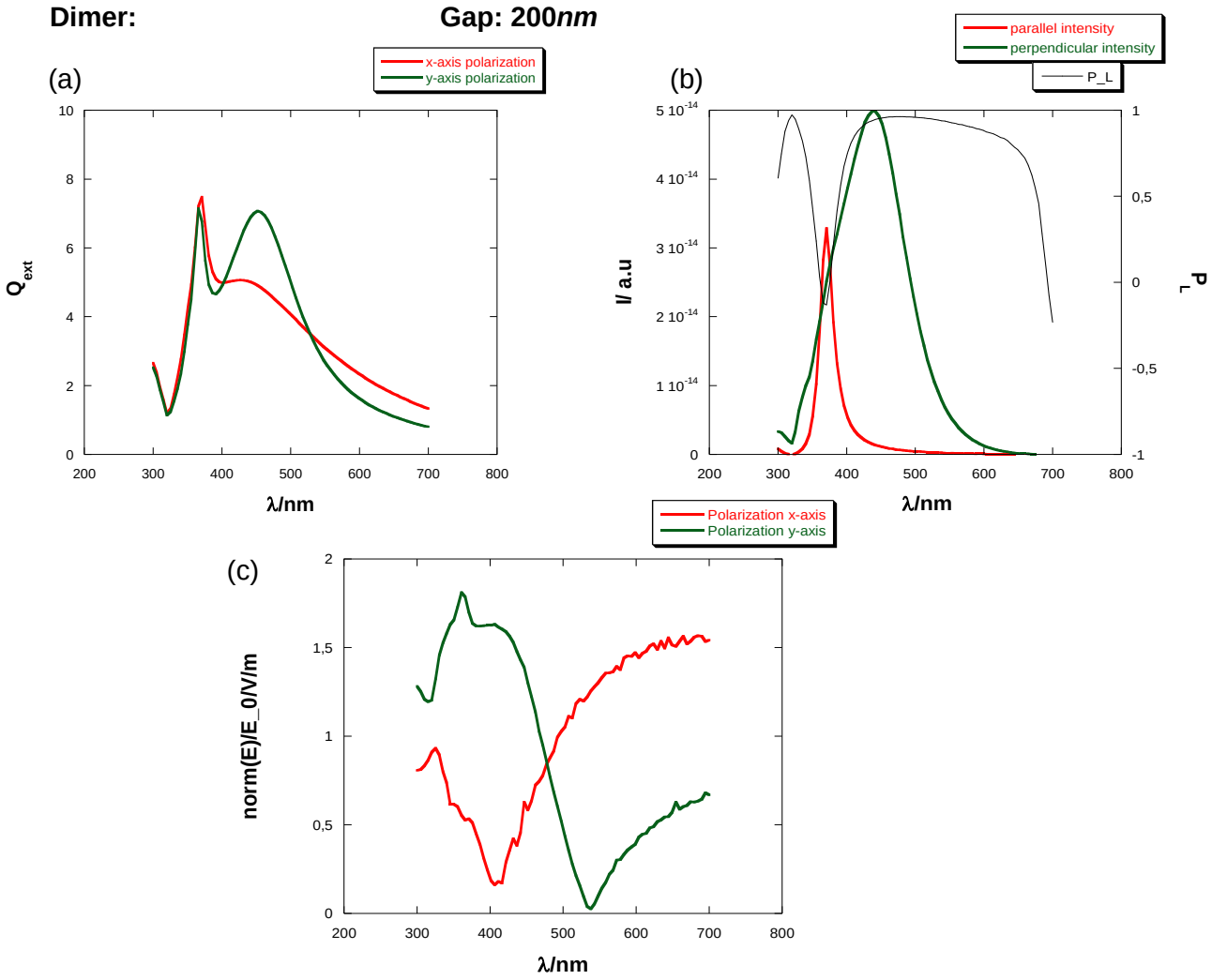

Figure 10.13: *(a) Extinction efficiencies. (b) Parallel and perpendicular intensities and $P_L(90º)$. (c) Norm of electric field in the center of gap.*

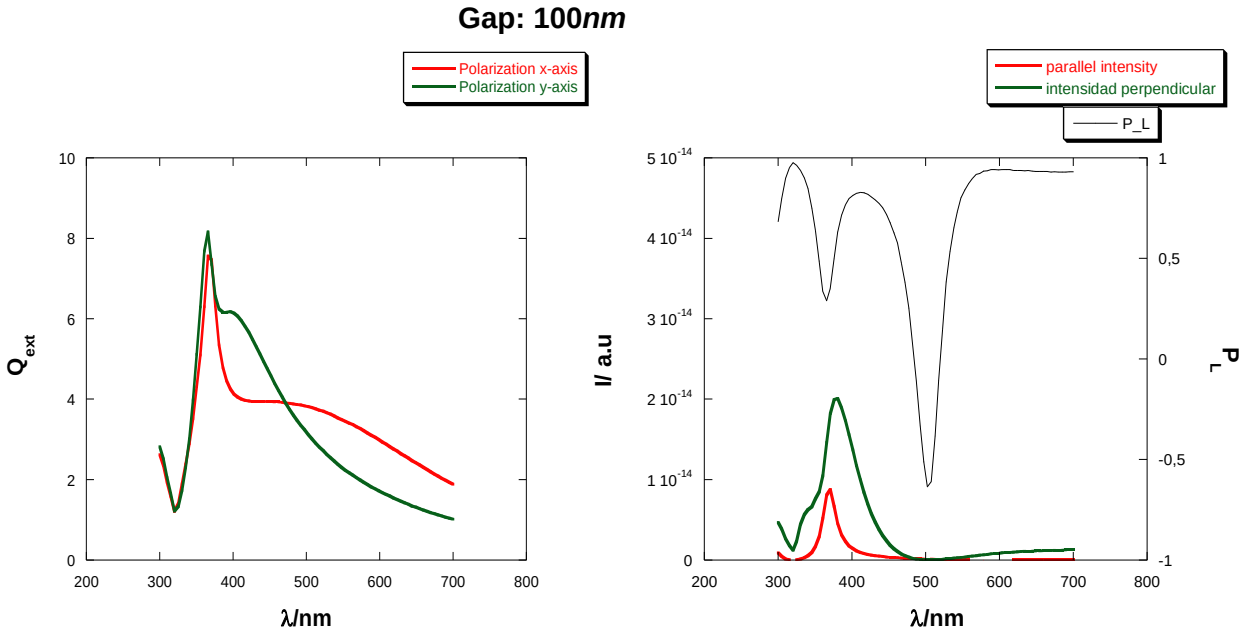

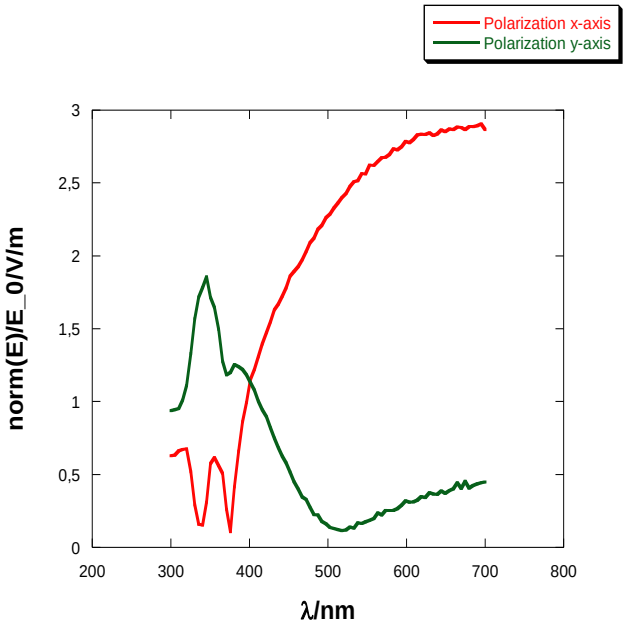

Figure 10.14: *(a) Extinction efficiencies. (b) Parallel and perpendicular intensities and $P_L(90º)$. (c) Norm of electric field in the center of gap.*

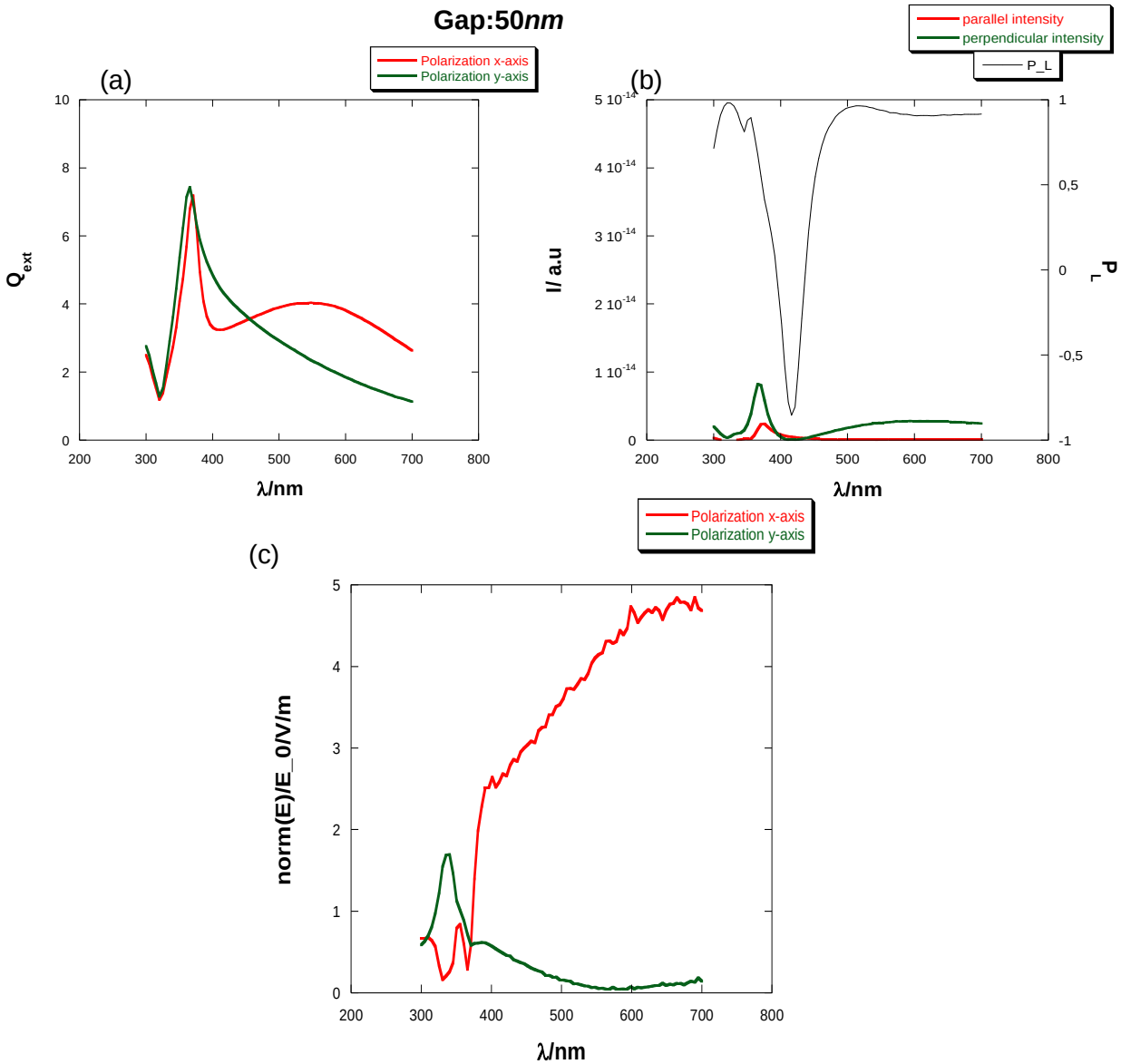

Figure 10.15: *(a) Extinction efficiencies. (b) Parallel and perpendicular intensities and $P_L(90º)$. (c) Norm of electric field in the center of gap.*

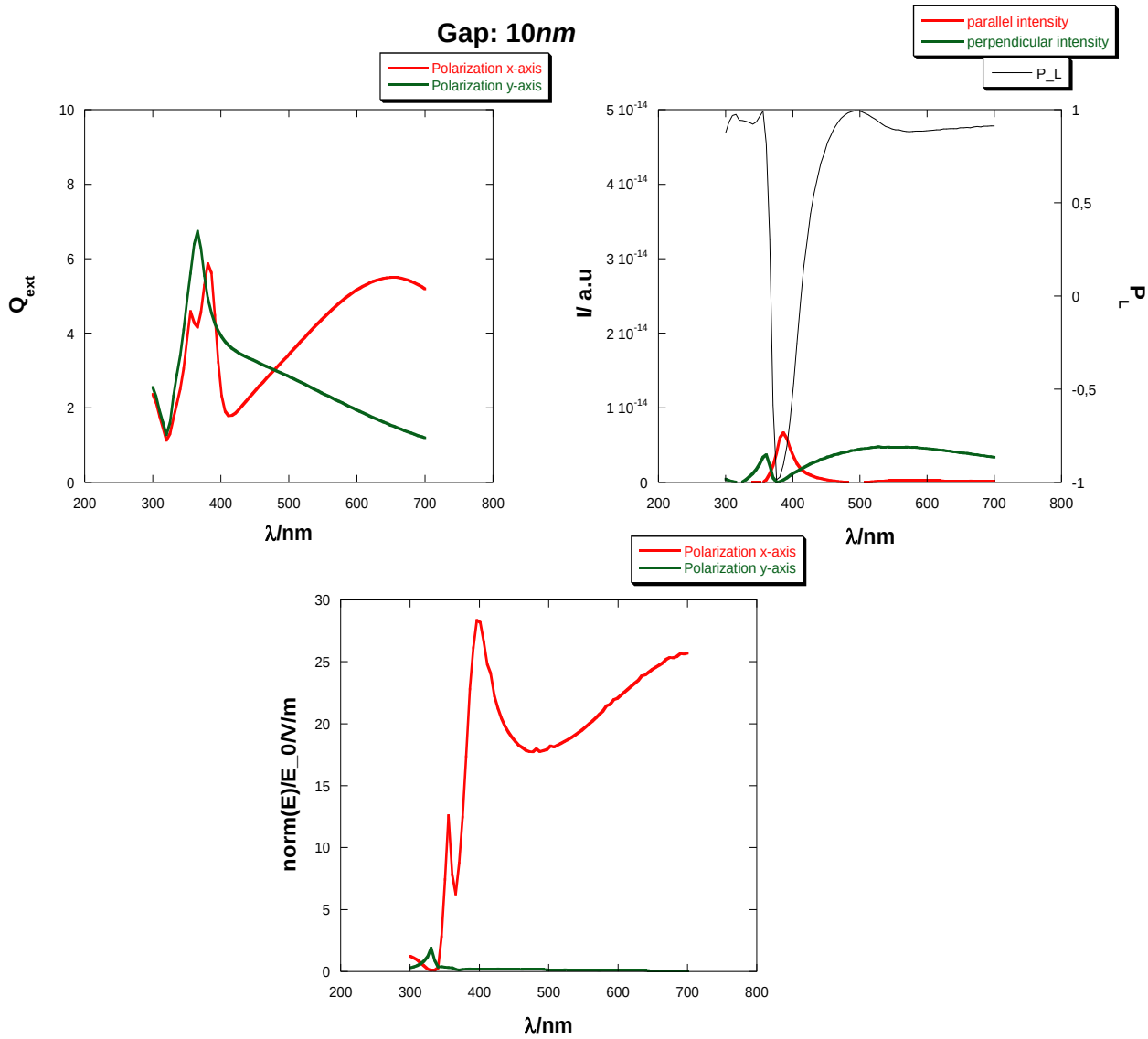

Figure 10.16: *(a) Extinction efficiencies. (b) Parallel and perpendicular intensities and $P_L(90º)$. (c) Norm of electric field in the center of gap.*

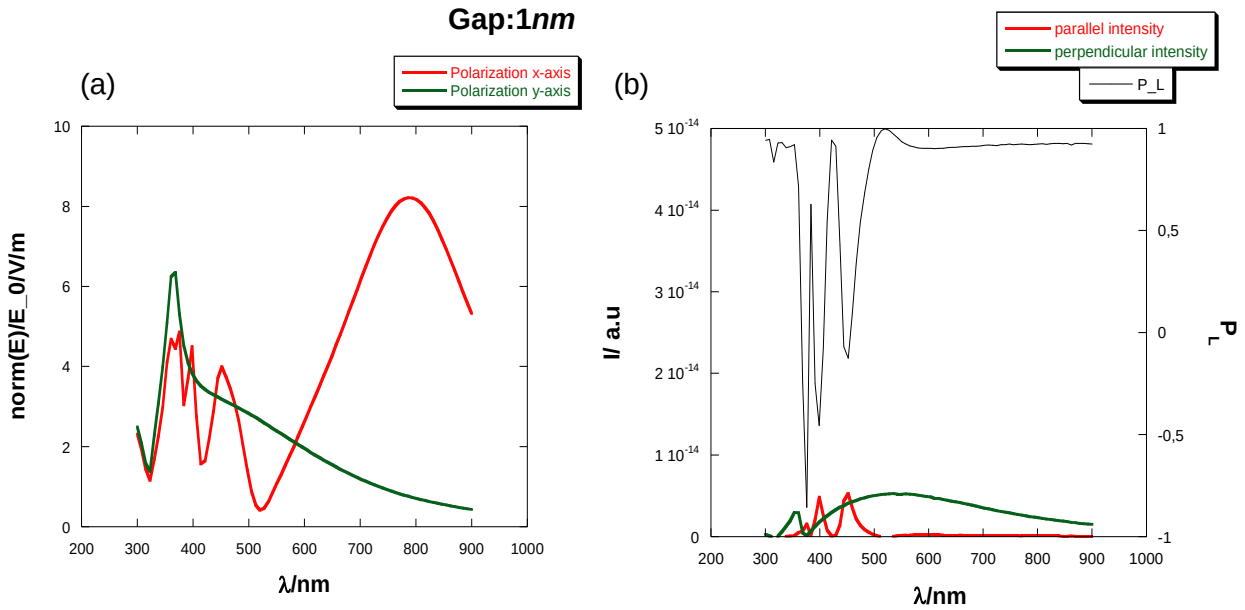

(c)

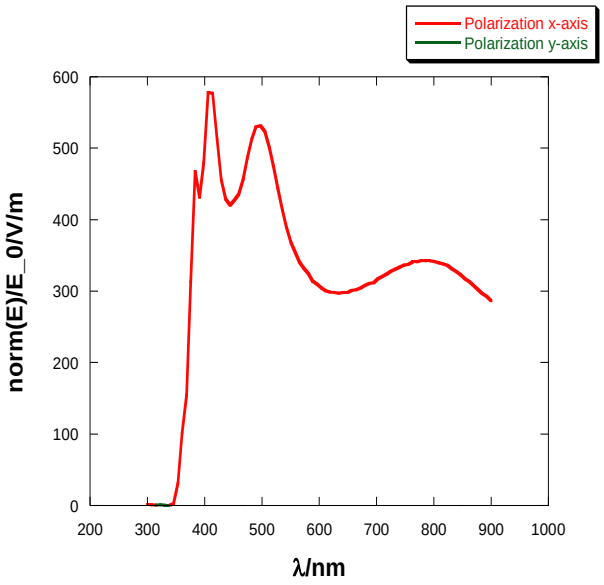

Figure 10.17: *(a) Extinction efficiencies. (b) Parallel and perpendicular intensities and $P_L(90º)$. (c) Norm of electric field in the center of gap.*

For the isolated particle in the extinction efficiency two peaks are shown. The highest corresponds to an electric quadrupolar charge distribution and the other one is due to an electric dipolar resonance. This can be observed through the values of the coefficients a_1, a_2, b_1, b_2.

For a gap corresponding to 200*nm* and polarization in x-axis (longitudinal configuration), we obtain very similar results for efficiencies as in case of the isolated particle. This is due to particles do not interact in far field. However, when light that illuminates particles is polarized in y-axis (transversal configuration), as a consequence of interaction in far-field between electric dipoles, dipolar electric term takes more importance. Perpendicular and parallel intensities appear to wavelengths where the electric dipolar and electric quadrupolar resonances are found, respectively. The P_L shows a minimum at the same position as the electric quadrupolar resonance.

The electric field norm in the center of gap shows a minimum due to interference effects. Also, it is not observed an enhancement because particles are very far each other.

Gap: 100*nm*. When incident light is polarized in x-axis, the electric quadrupolar term keeps the same values as in case of the isolated particle. However, the electric dipolar term, due to interaction between particles suffers a red-shift, broadens and its height decreases. This last effect is caused by the phase terms observed in the equation of the scattered electric field emitted by an electric dipole (7.1). Respect to polarization in y-axis, the dipolar term is less important for reasons explained before and a blue-shift is produced. The quadrupolar term appears to the same wavelength, although its height is slightly greater compared with the isolated particle.

In the P_L plot we can observe two peaks. One on the left appears due to the electric quadrupolar resonance, and the other one surges as a consequence of interference between light scattered by both particles.

Through the results of $\left|\vec{E}\right|$ we observe the same behavior as in the case of gap: 100*nm*.

In case of gap corresponding to 50*nm*, when we excite the system with light polarized in x-axis, we observe an extinction figure very similar to case of gap: 100*nm*. However, if we illuminate with light parallel to y-axis, the dipolar electric term almost disappears as a consequence of interaction between particles.

In the P_L we observe two peaks, the located one on the right in spectrum is caused by parallel intensity, which originates negative values of the linear polarization degree. Peak on the left is due to a greater difference between perpendicular and parallel intensities, although in this case, perpendicular intensity predominates over the parallel one. As we can see, it is repeated the same pattern as we obtained for gap: 100*nm*.

In the $\left|\vec{E}\right|$ we can see a similar plot that in the cases analyzed before.

Gap: 10*nm*. In case of polarization in x-axis, the electric dipolar term is shifted to longer wavelengths. Its extinction efficiency is slightly greater to gap corresponding to 50*nm*. This enhancement is due to interaction of dipoles in near-field, because in longitudinal configuration, they create a field in the same direction as polarization. The electric quadrupolar term is red-shifted and its height decreases. In spectrum appears a new peak, corresponding to the appearance of high order multipolar terms. In case of polarization along y-axis, we can observe a similar behavior to case of gap: 50*nm*, height of peak has diminished a bit.

In the P_L, we only see the electric quadrupolar contribution. The minimum reaches lower values, taking importance the magnetic effects.

In the $\left|\vec{E}\right|$ we observe a significant enhancement due to interaction effects between the two particles.

Gap: 1*nm*. When we illuminate particles with light parallel to the scattering plane, we can observe a red-shift of the electric dipolar term. Also, extinction efficiency is greater than in case of isolated particle. Motives of this increase are the same as those explained for gap of 10*nm*. For interaction the electric quadrupolar term is shifted to longer wavelengths and its height decreases. Furthermore, in spectrum new peaks appear, corresponding to high multipole orders. When the system is excited with light polarized in y-axis, we observe a similar spectrum to that got for a 10*nm* gap. Its height has diminished a bit more, although in this configuration, transversal, the interaction, in near field, is not as important as in longitudinal is.

In the P_L we observe three different peaks, the one located on the right gives information about the electric quadrupolar distribution, and the others are related with higher multipole orders.

The field in gap center is very high due to interaction. The maximum value found is the same as in case of the dimer r_1=10*nm*, r_2=10*nm*.

For illustrating the near field distribution for the cases analyzed before, we have created a map of near field which is included below. Two different situations have benn considered: when dimer is illuminated by a wavelength resonant corresponding to the electric dipole (a), and the electric quadrupole one (b).

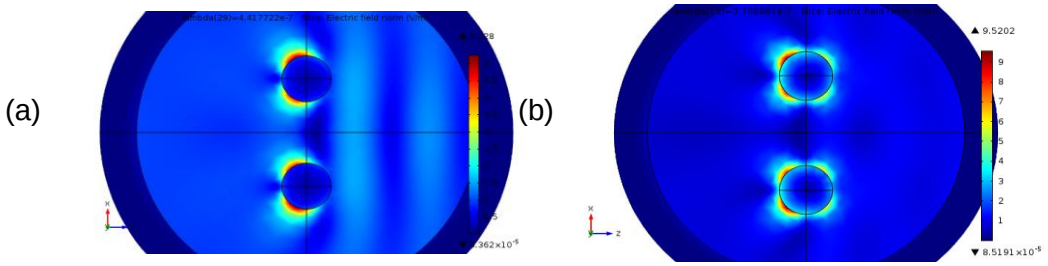

Figure 10.18: *Electric field norm. We illuminate the system with a plane wave, polarized in x-axis and propagating in –z-axis. Dimer is located in x-axis and size of components corresponds with: r_1=75nm r_2=75nm, particles are separated by 200nm. (a) Wavelength of incident radiation: 441nm, corresponding to an electric dipolar resonance. (b) λ=370nm, electric quadrupolar resonance.*

If we analyze the same cases, but with particles that constitute the dimer located in y-axis, in the extinction efficiency plots we can observe that outcomes obtained before for x-axis, in this new geometry, are obtained in y-axis, and vice versa. When system is illuminated with light polarized in x-axis we are in transversal configuration. However, when dimer is excited with electromagnetic radiation polarized in y-axis, longitudinal configuration is found. Considering particles placed in z-axis, we find the same results for both polarizations. This situation corresponds to transversal configuration.

Concerning to P_L analysis, we can observe the same results for cases in which particles are located in x-axis and in z-axis. This behavior is due to one particle covers to the other one when they are observed (x-axis) or when they are illuminated (z-axis). For y-axis different results are obtained. We decided to show in the work the configuration in which particles are placed in x-axis because we can study both polarizations parallel and perpendicular to the scattering plane and the possible retardation effects in the interference.

10.3 Dielectric dimer: Silicon

Isolated particle

First of all, we have studied the case of an isolated particle, whose radius was fixed to 150*nm*. Particle was supposed embedded in air. We have analyzed the efficiency plots (figure 10.19) and the linear polarization degree at 90º (figure 10.20).

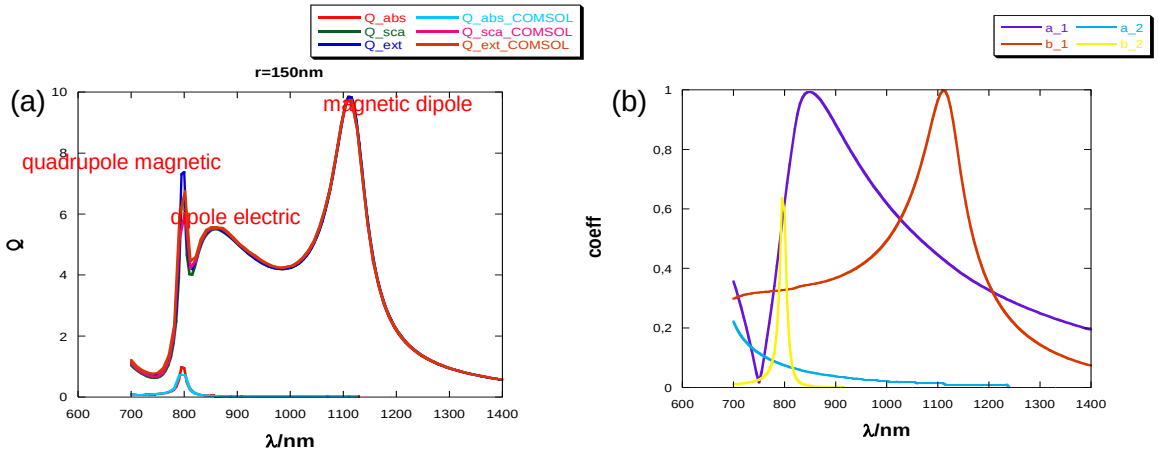

Figure 10.19: *a) Absorption, scattering and extinction efficiencies are shown, obtained with COMSOL and Matlab, for a silicon particle, r=150nm, when it is illuminated with*

light polarized in x-axis and propagating in z-axis. b) Contributions of electric dipolar, a_1, magnetic dipolar, b_1, electric quadrupolar, a_2, magnetic quadrupolar, b_2, terms.

From figure 10.19, we can see that, the first peak found in spectrum (looking from left to right side), corresponds to a magnetic quadrupolar resonance, the origin of the following one is electric dipolar and finally the last one is due to a magnetic dipolar effect. In view of P_L results, (figure 10.20), we can say that in wavelength where magnetic dipolar resonance takes place, the P_L reaches negative values. We must remark the appearance of two more peaks, which are close each other, and give information about the magnetic quadrupolar and electric dipolar contributions. Both take positive P_L values *[24]*, *[25]*.

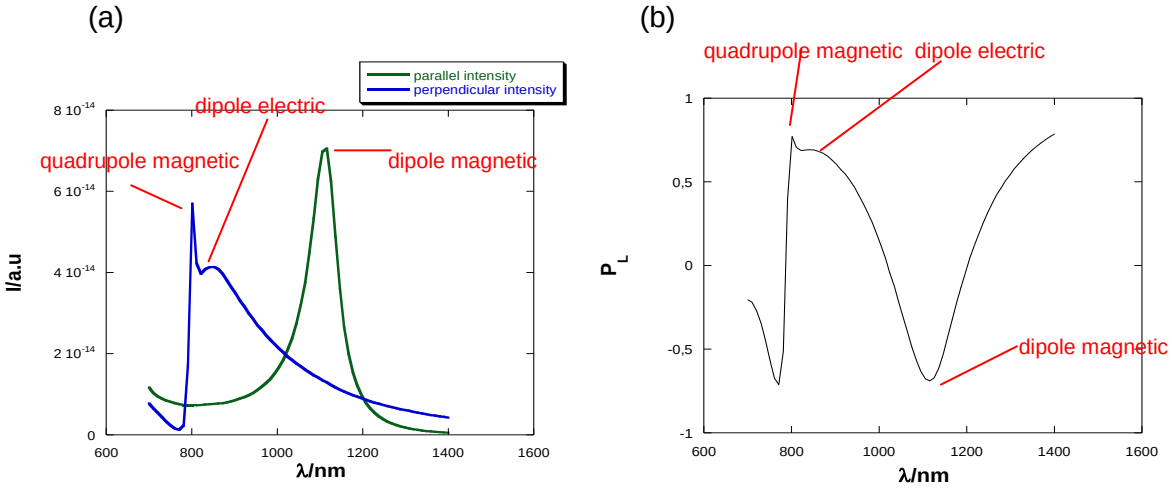

Figure 10.20: *a) Parallel and perpendicular intensities for case of an isolated silicon particle, r=150nm, when it is illuminated with a plane-wave, polarized in x-axis and propagating in z-axis. b) Linear polarization degree at 90°, (x-axis), versus wavelength.*

For dielectric dimer we have analyzed the same geometric configurations as in case of metallic dimers, explained before. Size of particles were fixed, in all cases, at 150*nm*.

Particles in x-axis.

We have analyzed the extinction efficiency plots (figure 10.21), linear polarization degree at 90º (figure 10.22), and near field maps (figure 10.23).

- **r_1=150*nm* r_2=150*nm***

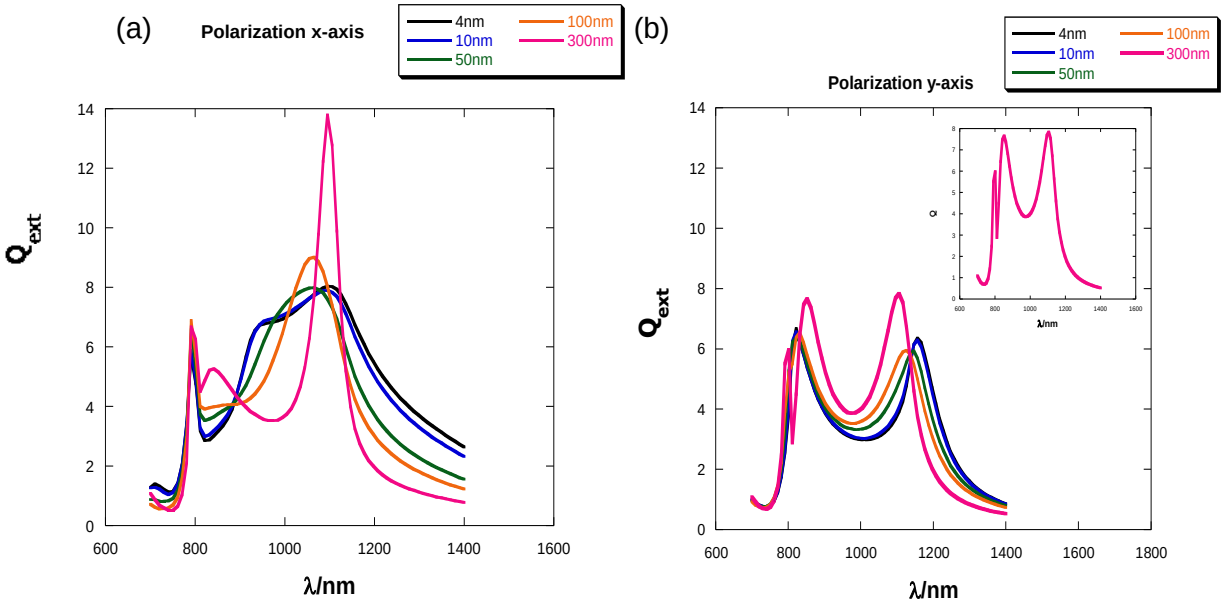

Figure 10.21: *Extinction efficiencies when a plane wave propagating in z-axis illuminates a silicon dimer. a) Incident radiation is polarized in x-axis. b) polarization y-axis, inside it, it is shown the extinction efficiency for a gap corresponding to 300nm.*

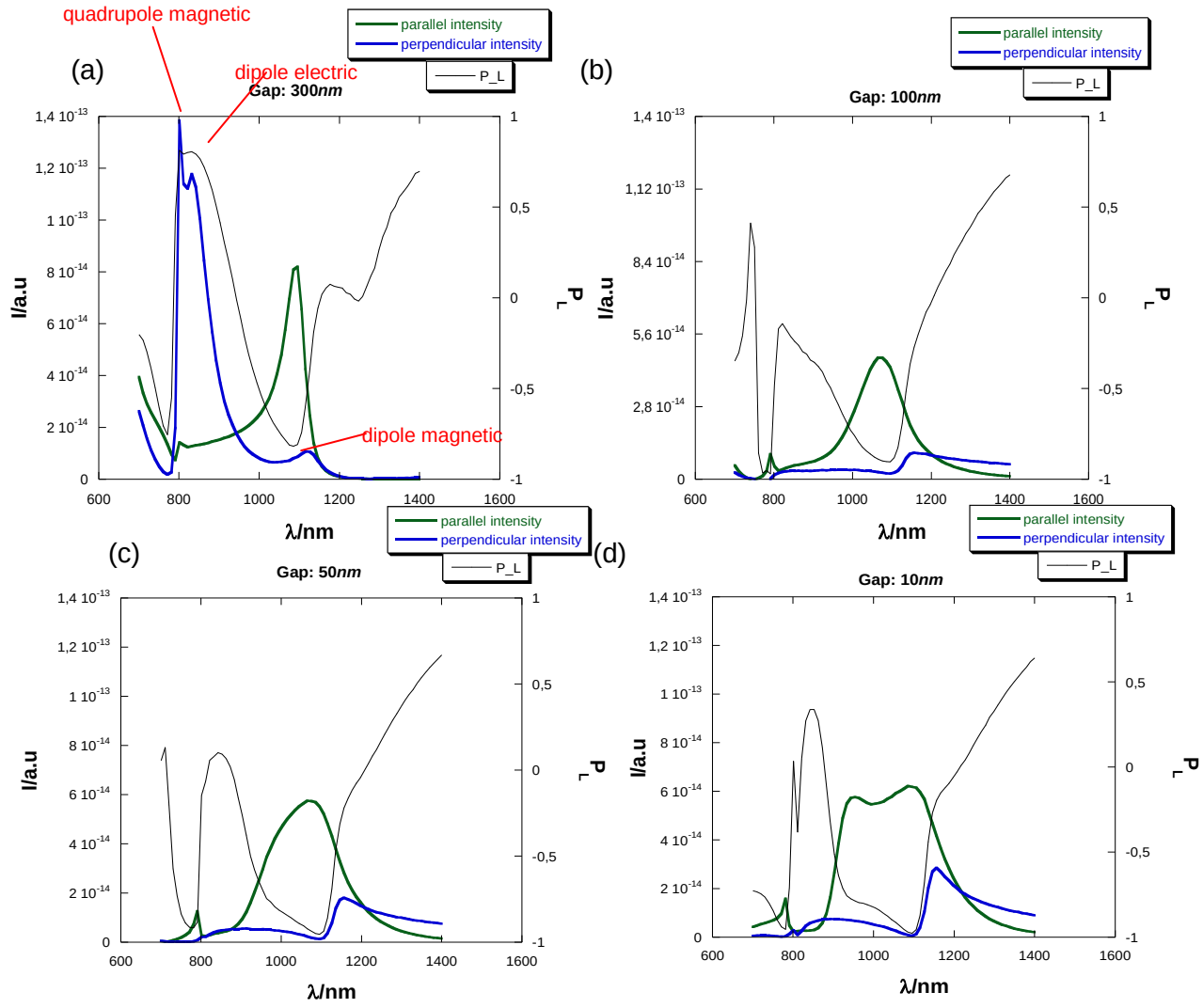

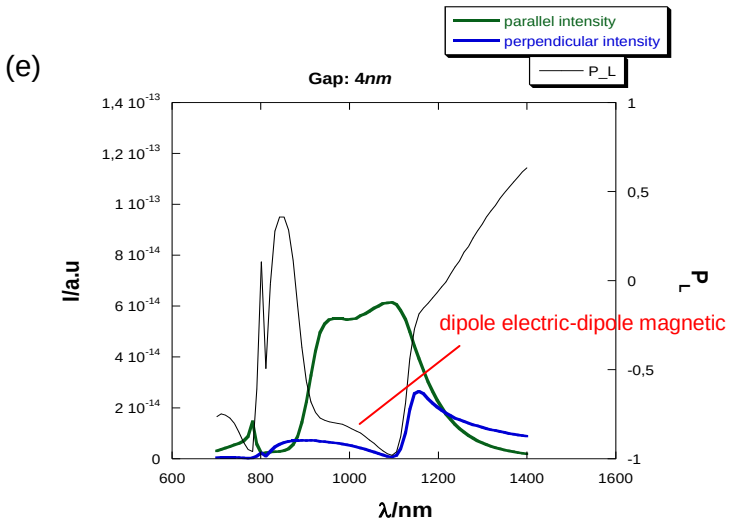

Figure 10.22: *Silicon dimer, r_1=150nm r_2=150nm, parallel and perpendicular intensities and linear polarization degree for the following gaps: a) 300, b) 100, c) 50, d) 10, e)4nm.*

In the figure 10.23 it is illustrated the electric field norm in near field. We can observe different oscillating modes of dipolar and quadrupolar fields.

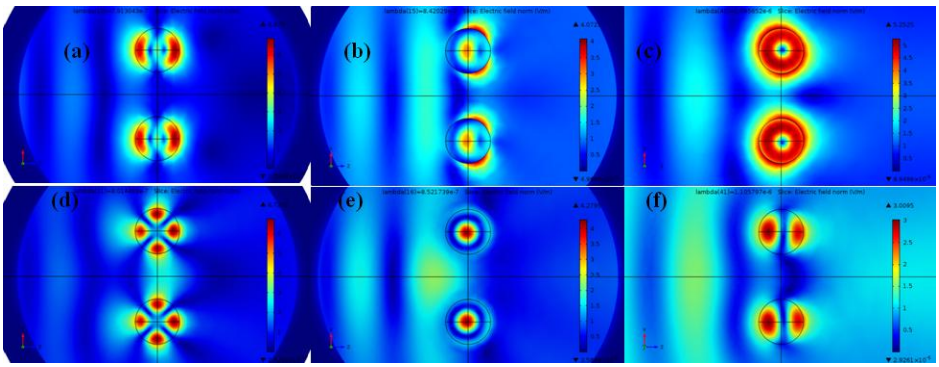

Figure 10.23: *Electric field norm for a Silicon dimer, r_1=150nm r_2=150nm and gap: 300nm. Particles are illuminated with polarized light in x-axis (images in upper row), in y-axis (images in bottom row), and propagating in z-axis. (a) System is excited with a wavelength corresponding to λ=791nm, it is observed the magnetic quadrupole. (b) λ=842nm, electric dipole. (c) λ=1095nm, magnetic dipole. (d) λ=801nm, magnetic quadrupole (e) λ=852nm, electric dipole. (f) λ=1105nm, magnetic dipole.*

As can be seen in figure 10.21 a), for polarization in x-axis and a gap corresponding to 300*nm* we observe in Q_{ext} the same contributions that we commented for isolated particle, however there are some differences, efficiency of the electric dipolar term is lower, this is due to interaction between electric dipoles. In longitudinal configuration and far field approximation interaction in line that joins both particles does not exit so we must consider complete expression of the electric field emitted by an electric dipole. In this situation phase terms are responsible for lower height of peak. For the magnetic dipolar contribution, occurs a similar effect to that explained before, however, in this case interaction occurs between magnetic dipoles. For gaps corresponding to 100 and 50*nm* we can see a similar behavior. As a consequence of the greater interaction,

electric dipolar resonance disappears. When particles are approximated, gap 10 and 4*nm* we find in Q_{ext} a new peak. This is due to interaction between electric dipole-electric dipole and electric dipole-magnetic dipole. [26]

For y-axis polarization, figure 10.21 b), gap 300*nm*, we can see the same charge distributions as in the case of isolated particle. However, for this polarization, the electric dipolar terms are blue-shifted, (transversal configuration), and the magnetic dipolar ones are red-shifted, (longitudinal configuration). Due to interaction between particles we can observe that the magnetic dipolar peak diminishes its height, while the electric dipolar increases it compared with the isolated particle. The magnetic quadrupolar term is given at the same wavelength, although its height is slightly lower. For a gap corresponding to 100*nm*, in Q_{ext} are shown only two peaks, this behavior is due to overlapping of the electric dipolar term with the magnetic quadrupolar one, the same plot is obtained for case of gap: 50*nm*. For gaps: 10, 4*nm* in extinction efficiency plots it is shown how the magnetic dipolar resonance suffers a red-shift, respect to the other gaps analyzed before, and the height of its peak increases. This effect is due to interaction between magnetic dipoles in near field.

In the analysis of the linear polarization degree at 90º we have only studied the dipolar range.

Through the linear polarization degree we can extract information about the origin of the different peaks that appear in extinction efficiency spectra. For gap corresponding to 300*nm* we can observe a minimum with negative values associated to the magnetic dipolar behavior. The obtained plot is similar to the case of the isolated particle. However, in this figure we observe fluctuations in $\lambda \sim$ 1200-1300*nm* due to interference effects. In case of gap corresponding to 100*nm* parallel intensity is the most important one, for this reason in the P_L we will find negative values. The magnetic dipolar behavior remains, even, it takes higher values. Nevertheless the electric dipolar contribution slightly disappears. Gap: 50*nm* we can observe a plot similar to that explained before. However, when the particles are closer each other, gap: 10*nm* the interaction between them increases, so that, the P_L takes a very different form, it is dominated by parallel intensity, the new term observed is due to the interaction between electric dipole-electric dipole and electric dipole-magnetic dipole. The same behavior is found for gap: 4*nm*.

Conclusions:

It has been carried out a study of the electromagnetic behavior of a dimer with two nanocomponents. In spectral extinction efficiency plots can be observed different resonances and how they change as a function of distance that separates the two constitutes of system. From the measurement of linear polarization degree we have extracted conclusions about the charge distributions that originate the resonances that are shown in spectrum.

We have developed a program with Matlab, in which Mie theory is summarized, with the objective of understanding the performance of the commercial software: COMSOL and comparing the results obtained with both programs.

Metallic particles:

For the case of silver nanoparticles, first of all, we have represented the plots corresponding to isolated particles. Through the graphics of first Mie coefficients can be explained the origin of peaks that appear in the efficiencies. It is observed that as the particle size increases the dipolar resonance is red-shifted, and peak broads. Also, more complex charge distributions are found. For small particles the absorption dominates over scattering, nevertheless, for big particles scattering is the most important effect.

In the results concerning to dimer, we can extract the following conclusions:

- For small particles compared with wavelength, the absorption dominates over scattering, nevertheless, for big particles scattering is the most important effect.

- For the smallest analyzed particle size, $r_1=r_2=20nm$, they behave as electric dipoles and the resonances can be described using the Drude-Lorentz model. For gaps corresponding to 200, 100 and 50*nm* in longitudinal configuration do not exit interaction and because of that in the efficiencies study is obtained the same result as in the case of isolated particle. However, in transversal configuration, in far-field dipoles interact each other. Gap: 10*nm* the near-field approximation can be considered, so that, in longitudinal configuration, interaction between electric dipoles originates an electric field in the same direction as the initial polarization of particle, which induce an increase in height of the peaks. For gap: 4*nm* it takes place a new contribution originated by the hybridization.

- In longitudinal configuration due to interaction a red-shift is observed, however, in the other situation a blue-shift is produced.

- For bigger particles, $r_1=r_2=150nm$ can be observed in spectrum a new peak corresponding to an electric quadrupolar charge distribution, in most of cases this peak is not shifted. Due to particle size, phase terms are present and are responsible for the value of the crests.

- For the latter particles P_L gives information about the estrangement of the dipolar behavior of system as it takes values smaller than 1. It indicates the presence of magnetic effects, acquiring negative values.

Dilectric particles:

- We can see as magnetic effects are important. In fact, in the isolated particle spectrum, two of the three contributions observed are magnetic. The resonances correspond with: magnetic quadrupolar, electric dipolar and magnetic dipolar charge distributions. For dimers we can observe as in transveral configuration when electric dipolar resonances are blue-shifted the magnetic ones are shifted to longer wavelengths. In the P_L plots appear negative values that give information about the magnetic contributions. The low absorption exhibited by these particles makes them very interesting in different devices, especially as nanoantennas.

- In the dipolar region the sign of P_L indicates if the electric term dominates or/and the magnetic one.

As conclusion, we would like to say that the system constituted by two nanoparticles, metallic or dielectric, is very useful for generating new resonances with high field values to different frequencies that in the case of isolated particles. Also, it is possible to produce hot-spots. All of these things are important in SERS technique, biosensors design, solar cells manufacturing, etc.

Future work

Concerning to future work, due to COMSOL potential other configurations, using different materials and geometric situations, can be analyzed. Here it is shown some projects that can be carried out.

- Analysis of complex geometries (aggregates, irregular particles…)

- In the case of dimers constituted by dielectric nanoparticles, we can analyze the Kerker`s conditions (zero forward, zero backward scattering).

- Inhomogeneous particles, like alloys, core-shell particles…

- Particles located onto substrate, analyzing the influence of size, shape, optics properties.

- Analyze nanoholes which present applications in plasmoninc biosensors.

Bibliography

[1] Heinz Raether. *Surface Plasmons on Smmoth and Rough Surfaces and on Gratings*. Springer-Verlag Berlin Heidelberg New York, 1988.

[2] F. J. García Vidal, L. Martín Moreno. Plasmones superficiales. *Investigación y ciencia*, **385**, 2008.

[3] M.I. Stockman. Nanoplasmonics: past, present, and glimpse into future. *Optics Express*, **119**, 2011.

[4] C. F. Bohren, D. R. Huffman, *Absorption and Scattering of Light by Small Particles*, John Wiley & Sons, 1983.

[5] J.M. Sanz Casado. *Polarimetría de Sistemas Difusores con Microestructuras: Efectos de Difusión Múltiple.* Ph. D Thesis Universidad de Cantabria, 2010.

[6] B. Setién, P. Albella, J.M. Saiz, F. González and F. Moreno. Spectral behavior of the linear polarization degree at right-angle scattering configuration for nanoparticle systems. *New Journal of Physics*, **12**, 2010.

[7] Paula Izquierdo Gómez. *Estudio electromagnético de nanopartículas multicapa*. Proyecto Fin Carrera, 2011.

[8] R. Gómez-Medina, Y.Zhang, M. Nieto-Vesperinas, J.J. Sáenz. Tractor beams for semiconductor spheres. *Nanospain,* 2013*.*

[9] G.W. Mulholland, C.F. Bohren, K.A. Fuller. Light Scattering by Agglomerates: Coupled Electric and Magnetic Dipole Method. *Langmuir*, **10**, 1994.

[10] R. Alcaraz de la Osa. *Nanostructured systems with arbitrary electric and magnetic properties: development and application of an extension of the discrete dipole approximation (E-DDA)*. Ph. D Thesis Universidad de Cantabria, 2013.

[11] F. Michael Kahnert. Numerical methods in electromagnetic scattering theory. *Journal of Quantitative Spectroscopy & Radiative transfer*, **79-80**, 2003.

[12] D.W. Mackowski, M.I. Mishchenko. A multiple sphere T-matrix fortran code for use on parallel computer clusters. *Journal of Quantitative Spectroscopy & Radiative transfer*, **112**, 2011.

[13] J. Zhao, A.O. Pinchuk, et al. Methods for Describing the Electromagnetic Properties of Silver and Gold Nanoparticles. *Accounts of chemical research*, **41**, 2008.

[14] M.I. Stockman. Nanoplasmonics: The Physics behind the applications. *Physics Today*, **64**, 2011.

[15] X. Chen, H.J. Schlvesser. Nanosilver: a nanoproduct in medical application. *Toxicology Letters*, **176**, 2008.

[16] V. Giannini, A.I. Fernández-Domínguez, S.C. Heck, and S.A. Maier. Plasmonic Nanoantennas: Fundamentals and Their Use in Controlling the Radiative Properties of Nanoemitters. Chemical Reviews, **111**, 2011.

[17] T. L. Paxon, R. Scott et al. Identifying biological agents with surface-enhanced Raman Scattering. *SPIE Newsroom*, 2011.

[18] S. Person, M. Jain, et al. Demonstration of zero optical backscattering from single nanoparticles. *Nano Letters,* **13**, 2013.

[19] J.M. Aunón and M. Nieto-Vesperinas. Forces between a partially coherent fluctuating source and a magnetodielectric particle. arXiv:1303.4545 *Physics.optics ,* 2013.

[20] Y.X. Ni, L. Gao, A.E. Miroshnichenko and C.W. Qiu. Controlling light scattering and polarization by spherical particles with radial anisotropy, *Optics Express*, **21**, 2013.

[21] Y.H. Fu, A.I. Kuznetsov, et al. Directional visible light scattering by silicon nanoparticles. *Nature Communications*, **4**, 2013.
[22] W. Rechberger, A. Hohenau, et al. Optical properties of two interacting gold nanoparticles. *Optics Communications*, **220**, 2003.
[23] P. Noardlander, C. Oubre, E. Prodan, K. Li and M.I. Stockman. Plasmon hybridization in Nanoparticle Dimers. *Nano Letters*, **4**, 2004.
[24] R. Gómez-Medina, B. García-Cámara, I. Suárez-Lacalle, F. González, F. Moreno, M. Nieto-Vesperinas. Electric and Magnetic dipolar response of germanium nanospheres: interference effects, scattering anisotropy, and optical forces. *Journal of NanoPhotonics*, **5**, 2011.
[25] A. García Etxarri, R. Gómez-Medina, et al. Strong magnetic response of submicron Silicon particles in the infrared. *Optics Express*, **19**, 2011.
[26] P. Albella, M. A. Poyli, et al. Low-Loss Electric and Magnetic Field-Enhanced Spectroscopy with Subwavelength Silicon Dimers. *The Journal of Physycal Chemistry*. 2013. DOI: 10.1021/jp4027018I
[27] A. Dogariu, S. Sukhov, J.J. Sáenz. Optically induced 'negative forces'. *Nature Photonics*, **7**, 2013.
[28] R. Alcaraz de la Osa, J.M. Sanz, J.M. Saiz, F. González and F. Moreno. Quantum optical response of metallic nanoparticles and dimers. *Optics Letters*, **37**, 2012.

List of figures: